Heliyon 10 (2024) e38299

Contents lists available at ScienceDirect

Heliyon

journal homepage: www.cell.com/heliyon

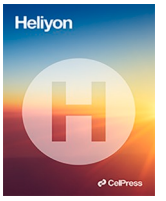

Research article

# Evaluation of entropy-coupled multi-criteria decision-making methods for enhancing machinability

Nafisa Anzum Sristi *, Prianka B. Zaman, Nikhil R. Dhar

*Department of Industrial and Production Engineering, Bangladesh University of Engineering and Technology, Dhaka, 1000, Bangladesh*

ARTICLE INFO

*Keywords:*
Turning
Taguchi
Entropy
MCDM methods
Machinability

ABSTRACT

Optimizing machining parameters is crucial, enhancing machinability while maintaining high product quality standards. This study bridges a critical research gap by evaluating and comparing five Taguchi-based Multi-Criteria Decision Making (MCDM) techniques—Combined Compromised Solution (CoCoSo), Grey Relational Analysis (GRA), Multi-Objective Optimization Ratio Analysis (MOORA), Technique for Order Preference by Similarity to Ideal Solution (TOPSIS), and Complex Proportional Assessment (COPRAS)—coupled with the Entropy method to optimize machining parameters for enhancing machinability in turning medium carbon steel. The focus is on feed rate and cutting speed under dry and Minimum Quantity Lubrication (MQL) environments considering six critical machining responses: material removal rate, surface roughness, main cutting force, cutting temperature, cutting ratio, and tool life.

The results reveal that MQL consistently improves machining performance, with COPRAS, TOPSIS, MOORA, and GRA converging on an optimal setting favoring an MQL environment, a 0.14 mm/rev feed rate, and a cutting speed of 137 m/min, whereas CoCoSo suggests a different optimal parameter setting. CoCoSo and GRA demonstrate the highest reliability, evidenced by minimal discrepancies between predicted and experimental results, with absolute percentage errors of 0.647 % and 0.659 %, respectively. The COPRAS method also shows strong predictive accuracy with a 5.573 % error, outperforming MOORA and TOPSIS. Spearman's rank correlation analysis reveals a high agreement between COPRAS, MOORA, and TOPSIS, with COPRAS emerging as a potential replacement for the latter in similar decision-making scenarios. SEM and EDX analyses confirm that MQL conditions reduce tool wear, enhance surface quality, and extend tool life compared to dry machining. This research provides insights into effective parameter optimization strategies for improving machinability and underscores the benefits of adopting MQL for sustainable manufacturing processes.

## 1. Introduction

Turning is a widely utilized machining process that involves the use of single-point cutting tools to shape workpieces. This process is particularly valued for its ability to produce complex geometric forms with high precision, making it essential in various industrial applications [1]. Despite its benefits, turning faces significant challenges, primarily due to the cutting zone's friction and heat generation, which can adversely affect the quality of the machined parts and tool life. Different cooling techniques have been developed to

* Corresponding author.
*E-mail address:* sristi094@gmail.com (N.A. Sristi).

https://doi.org/10.1016/j.heliyon.2024.e38299
Received 3 July 2024; Received in revised form 31 August 2024; Accepted 20 September 2024
Available online 21 September 2024

mitigate these effects. Cutting fluid is mainly directed at the chip-tool interface to diminish friction and cutting forces, extending tool longevity by effectively cooling the cutting area [2,3]. Typically, the type of coolant or cooling strategy influences the energy required to cut a specific volume of material. The formation of built-up edges and tool life are primarily determined by cooling conditions rather than other factors [4].

While cutting fluids are effective in cooling and lubrication, they often contain hazardous chemical constituents that pose significant environmental and health risks [5,6]. Alternative cooling methods, such as dry and MQL [7], have been explored to address these concerns. MQL, in particular, has gained attention for its ability to lessen the application of cutting fluids, promoting a greener process. MQL helps lower the temperature at the tooltip, reduces cutting forces, and enhances the machined components' surface quality and tool longevity [8,9]. MQL significantly improves the machinability index with minimal investment costs [10]. MQL enhances machinability by effectively delaying the adhesion of chips to the edge of the cutting tool [11]. The use of MQL in machining processes shows considerably greater effectiveness in reducing flank wear compared to dry conditions [12]. Ross et al. [13] assessed the heat-carrying capacity of the Minimum Quantity Lubrication (MQL) system and the impact of nano-additives on its cooling efficiency. The results confirmed that using nano MQL in machining led to an average temperature reduction of approximately 65 % compared to conditions without coolant. Gupta et al. [14] utilized a fundamental conceptual framework for sustainability assessment to improve the machining performance of Bohler K490 steel using minimum quantity lubrication (MQL). They asserted that MQL enhances both sustainability and machining effectiveness. Maruda et al. [15] examined the surface integrity of AISI 1045 steel during turning with minimum quantity lubrication and found that using MQL led to a uniform distribution of valleys and peaks on the turned surface.

Additionally, optimization of the turning process is crucial to achieve increased machinability [16]. The Taguchi method is widely used for process optimization due to its efficient design of experiments (DoE) and computational simplicity [17]. However, the standalone Taguchi method cannot address multiple objectives simultaneously. Hybrid optimization techniques have been developed to overcome this limitation, integrating the Taguchi method with other multi-response optimization methods [18]. These hybrid methods allow for accommodating multiple conflicting criteria in the decision-making process. It is crucial in industrial applications where various performance aspects like surface quality, tool longevity, and machining effectiveness need simultaneous optimization to enhance machinability.

TOPSIS can do multi-optimization, but assigning equal importance to all criteria is not feasible [19]. Therefore, determining the appropriate weights for the criteria is crucial. Methods for determining these weights fall into two categories: subjective and objective. Objective methods calculate weights using experimental data rather than relying on expert opinions [20]. Well-known objective methods incorporate the CRITIC method (CRiteria Importance Through Intercriteria Correlation), Entropy method, FANMA method (named after its authors), and Data Envelopment Analysis (DEA). Arun Prasad et al. [21] employed the Entropy technique to find the importance of output responses and applied these weights to the multi-optimization process. The Entropy method evaluates the uncertainty of data in the decision matrix and generates weight coefficients based on the mutual contrast of individual criterion values for each alternative and then for all criteria. The Entropy method is widely employed due to its straightforward, impartial, and uncomplicated calculation of the relative importance of responses [22].

Nguyen et al. [23] investigated the influence of the MQL condition during milling of the Ti-6Al-4V alloy, optimizing production rate and surface roughness using the TOPSIS method. Balasubramaniyan et al. [24] employed turning parameter optimization of EN25 steel using TOPSIS. Thirumalai et al. [25] utilized the TOPSIS approach to perform turning parameters optimization of Inconel 718. Gupta et al. [26] determined optimal turning parameters for Ti–6Al–7Nb by TOPSIS under an MQL environment, considering different input process variables such as the type of oil, the oil flow rate, and the cutting speed. Do et al. [27] applied CoCoSo for the first time in machining processes to prioritize the solutions for AISI 1045 steel in hole turning. Abbed et al. [28] employed different MCDM methods for optimizing the turning parameters of Ti-6Al-4V under dry conditions and found that the CoCoSo method effectively minimized force, tool wear, and power consumption. Yurtkuran et al. [29] used various machine-learning models to predict power consumption during the milling of Ph13-8Mo steel. Their findings indicated that power consumption rose by an average of 3.14 % across all cutting environments as feed speed increased.

Patil et al. [30] used the COPRAS MCDM optimization technique to find optimum machining parameters for OHNS steel with 55 HRC, considering factors such as nose radius, insert type, depth of cut, speed, and feed. Krishna et al. [31] utilized MOORA and COPRAS methods, combined with the entropy technique, to optimize the turning parameters for Nimonic C263 in dry conditions. Das et al. [32] employed GRA, VIKOR, and MOORA techniques to analyze the effect of depth of cut, feed, and speed on the material removal rate and surface finish while turning a Cu–Ni alloy with a carbide cutting tool. Their findings indicate that all MCDM techniques consistently show that the optimal compromise is achieved at the highest levels of parameters. Solanki et al. [33] found that TOPSIS and GRA methodologies effectively identify optimal process parameter combinations for turning Al-6082 under wet conditions. These methodologies consider depth of cut, feed rate, and cutting speed to achieve the best combination of surface roughness and material removal rate. Sarıkaya et al. [34] conducted experiments on turning the cobalt-based superalloy Haynes 25 to identify optimal MQL parameters using Taguchi-coupled GRA approach. Singaravel et al. [35] applied the MOORA method combined with the entropy method to optimize turning parameters for EN25 steel. Jeet et al. [36] attempted to determine optimal cutting conditions during machining EN-24 steel under three different cutting conditions by MOORA, TOPSIS, and GRA methods considering equal weightage of each response. Abhang et al. [37] discovered that the optimal outcomes identified through GRA coincided precisely with those achieved using the MOORA method, emphasizing that MOORA relies solely on straightforward ratio analysis rather than the more complex GRA. Bag et al. [38] analyzed the turning of EN8 steel with an HSS S200 tool to achieve maximum material removal rate (MRR) and minimal tool wear using Taguchi-based optimization techniques, including TOPSIS, GRA, and ARAS methods. The results showed that the optimal parameter settings for both TOPSIS and GRA were the same: a spindle speed of 210 rpm, a feed rate of 0.142

mm/rev, a depth of cut of 1.5 mm, and soybean oil as the cutting fluid. Hadjela et al. [39] conducted a turning experiment on AISI 4140 alloy steel to determine the cutting conditions that would minimize surface roughness and flank wear while maximizing the material removal rate. They used various optimization methods, including Taguchi-based GRA, TOPSIS, and MOORA. All three multi-objective optimization techniques identified the same optimal cutting conditions.

Furthermore, tool wear is closely linked to efficient operation, quality, dimensional accuracy of the workpiece, and tool lifespan. The practical evaluation of friction forces and cooling conditions enables the timely replacement of materials before catastrophic failure occurs [40]. Predicting wear using friction forces under various cooling conditions through intelligent techniques is crucial. Korkmaz et al. [41] investigated tool wear when turning AA7075 aluminum alloy at various speed-feed settings. Their findings revealed a 44.40 % increase in tool wear when the cutting speed was doubled while feed rates remained constant. Additionally, higher feed rates result in a longer cutting-edge travel distance within a given time, leading to a larger cutting surface area and, consequently, increased cutting force. The impact of the cooling environment on tool wear is a crucial factor that requires further analysis in the future.

After reviewing the literature, it is evident that significant research has been conducted on optimizing machining parameters concerning only two or three machining responses across various cooling environments. However, to ensure effective machinability improvement, it is vital to consider several machining responses instead of two or three to get accurate and reliable decisions regarding optimal machining parameter selection. Additionally, the efficiency, reliability, and effectiveness of different MCDM methods should be analyzed and compared in terms of machining performance concerning material and other resource wastage, and the proper selection of the MCDM method for process optimization can ensure this. However, there is a noticeable gap in the literature concerning the evaluation and comparison of various Taguchi-based MCDM methods—specifically CoCoSo, GRA, MOORA, TOPSIS, and COPRAS—in enhancing machinability. Despite the superior performance of these methods, their comparative effectiveness has been underexplored. Moreover, the impact of the cooling environment on tool wear and life is a critical factor that requires further comprehensive analysis to ensure sustainability.

The current article concentrates on the critical question: How can optimizing process parameters effectively balance essential machining responses to achieve desired machinability while promoting sustainable manufacturing processes?

This study focuses on employing various Taguchi-based Multi-Criteria Decision Making (MCDM) methods—CoCoSo, GRA, MOORA, TOPSIS, and COPRAS—to optimize feed rate and cutting speed to enhance machinability regarding six machining responses—material removal rate, surface roughness, main cutting force, cutting temperature, cutting ratio, and tool life for turning medium carbon steel using an uncoated carbide insert. The investigation encompasses two distinct cooling environments: Minimum Quantity Lubrication (MQL) and dry. The entropy method, renowned for its objective approach, will be utilized to assign weights to the different responses observed during the turning process. By evaluating and comparing the outcomes derived from these five MCDM methods, this study aims to identify the optimal turning parameters to enhance machinability through extensive exploration. A confirmation test will be performed to verify the reliability of the MCDM methods. Moreover, these optimal parameters could provide a valuable reference for future turning operations, potentially eliminating the necessity for extensive trial experiments. Additionally, SEM (Scanning electron microscopy) and EDX (Energy-dispersive X-ray) analysis of the carbide insert will be conducted under both cooling environments to comprehensively understand their effects on tool wear and lifespan, contributing to sustainable manufacturing processes.

## 2. Experimental overview

### 2.1. Process specifics and materials

A 10-horsepower Center lathe (China) was used to conduct the turning experiments. Medium carbon steel was utilized as the work material; its properties are detailed in Table 1. An uncoated tungsten carbide insert, SNMM 120408 (ISO P30 grade), served as the cutting tool insert, featuring the following geometry: 6°, −6°, 6°, 15°, 75°, 0.8 mm. A WIDIA tool holder with the ISO specification PSBNR 2525 $M^{12}$ was utilized for turning experiments, following recommended speed-feed combinations suggested by the manufacturer for standard industrial applications. Uncoated carbide inserts were selected for their low cost, availability, and time efficiency [42]. Because the depth of cut has a minimal impact on cutting temperature, preserves work material, and avoids significant influence from the nose radius on cutting temperature, a constant depth of cut of 1.5 mm was maintained throughout the experiments [43], which was suitable for the study's objectives.

Fig. 1(a) illustrates the experimental setup, including the Minimum Quantity Lubrication (MQL) system used in this study. The MQL delivery system comprises a compressor, fluid chamber, and mixing chamber with a nozzle. A pressure regulator and flow meter are positioned to control pressure and flow rate—the compressor, which can generate a maximum pressure of 25 bars, supplies

**Table 1**
Characteristics of the workpiece used.

| Workpiece | Hardness (BHN) | UTS (Kgf/mm$^2$) | Thermal conductivity (W/mm K) | Chemical composition (wt %) |
|---|---|---|---|---|
| Medium carbon steel | 180 | 63 | 0.036 | Mn: 0.60<br>C: 0.38<br>S: 0.01<br>P: 0.01 |

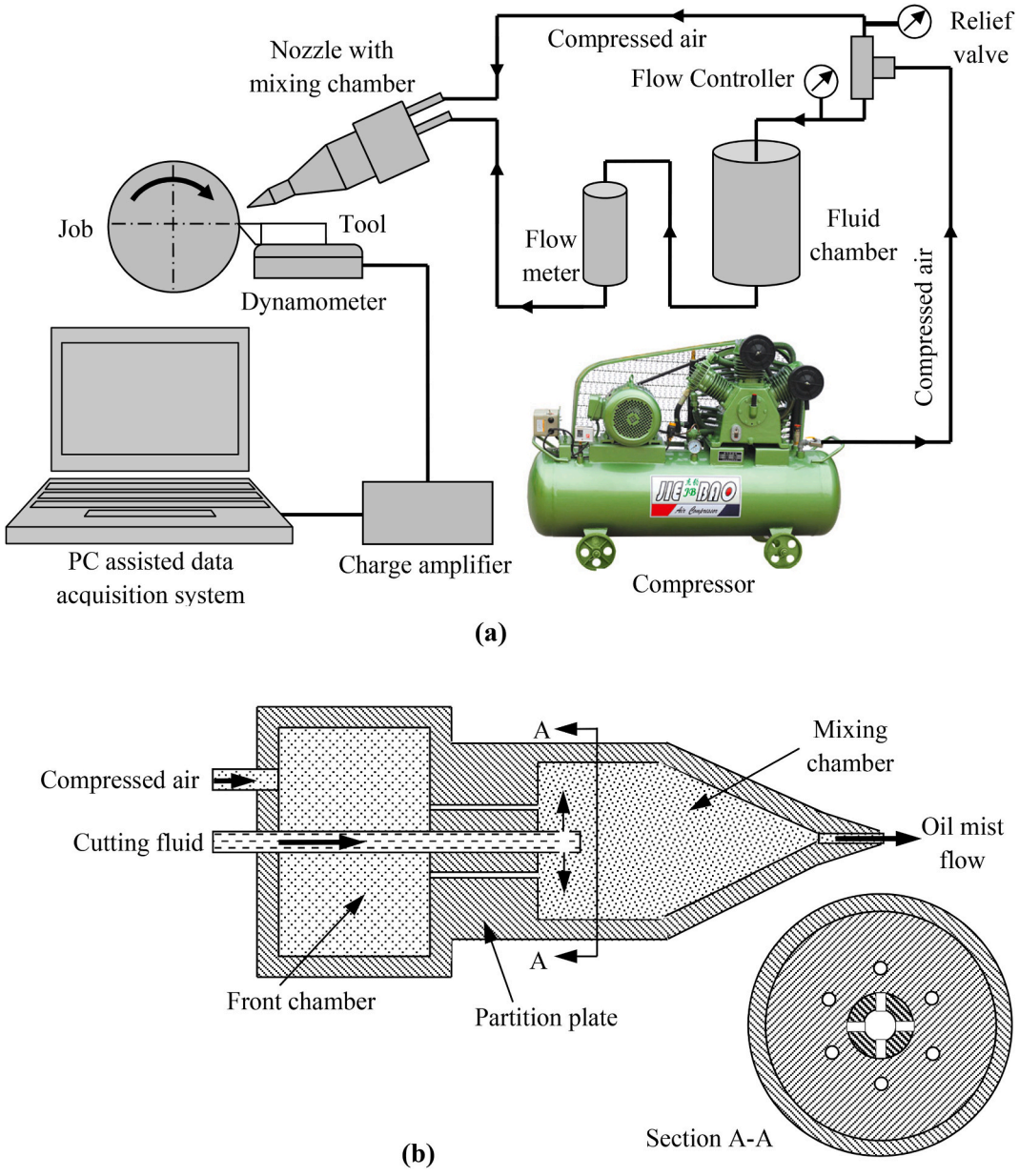


**Fig. 1.** (a) Diagram of the experimental setup with (b) Details of the MQL applicator and nozzle specifications.

compressed air. A cutting fluid (1:20 soluble oil) is applied at a 200 ml/h flow rate through an external nozzle. Compressed air is divided between the mixing chamber and the fluid chamber; some air flows directly into the mixing chamber, while the rest moves through the fluid chamber to push the fluid toward the mixing chamber. The fluid chamber has a capacity of 1 L. Air and oil are combined in the mixing chamber to create an air-oil mist. Oil enters the mixing chamber through a central tube and exits through small radial holes at the tube's end. Air enters through an inlet tube and passes through holes in the partition plate, mixing with the oil perpendicularly to form the mist. The tapered design of the mixing chamber helps direct the mist to the nozzle connected to its outlet port. Details of the mixing chamber and its sectional view are shown in Fig. 1(b).

### *2.2. Machining response measurements*

During each experimental trial, cutting temperature (T) was monitored using a thermocouple tailored for the specific tool-work material combination, with the tool and workpiece acting as two dissimilar metals. Two copper wires connected the tool to a distant workpiece section, routing through a multimeter to close the thermoelectric circuit. A copper rod attached to a wire touched the workpiece, serving as the cold junction (room temperature), and the hot junction formed at the chip-tool interface during machining.

Insulating the tool and workpiece from the lathe machine was essential, achieved using leather for the workpiece and a mica sheet for the tool holder. Although this technique measures the average cutting temperature over the entire contact area and not high local temperatures, it is a simple and reliable method for a wide temperature range [44]. Fig. 2(a) illustrates the measurement setup for cutting temperature using this tool-work thermocouple system. To use the tool-work thermocouple technique for temperature measurement, proper calibration is necessary to correlate the generated voltage with the actual temperature for the specific tool-work material combination. For this calibration, a long tubular chip and a tungsten carbide rod were brazed together at one end, substituting for the work material and tool insert. A half-spherical graphite block, seated on porcelain and electrically heated, acted as the heat source. The brazed junction of the tool-work thermocouple and a standard chromel-alumel thermocouple were placed side by side in the graphite block. The free ends of the chip and tungsten carbide rod were connected to a digital multimeter (Rish Multi 15S, India). Fig. 2 (b) shows a photographic view of the study's setup used for tool-work thermocouple calibration. As the graphite block was heated, the tool-work thermocouple generated a thermoelectric voltage recorded by the multimeter. Simultaneously, a digital

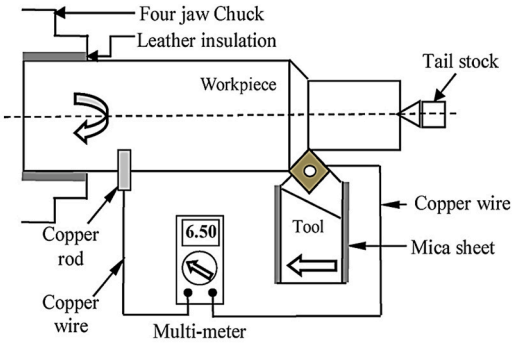


(a)

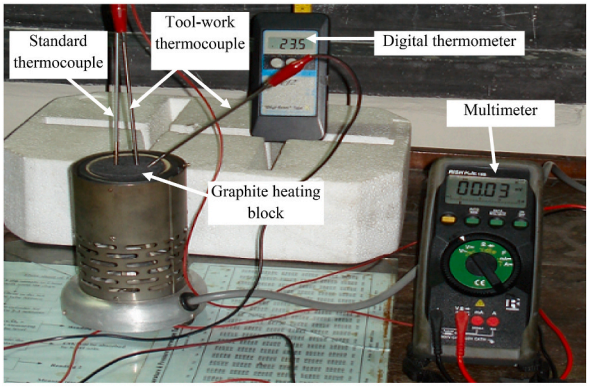


(b)

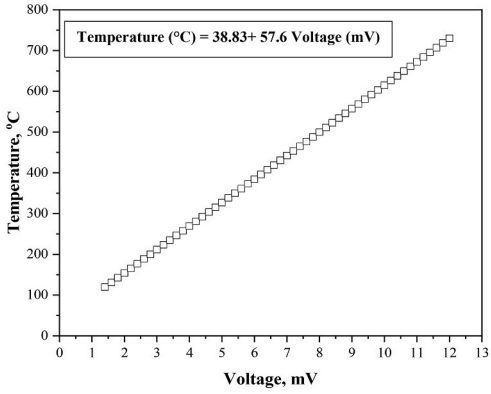


(c)

**Fig. 2.** (a) Setup for measuring cutting temperature through the tool-work thermocouple system, (b) Calibration setup for the tool-work thermocouple, and (c) Calibration curve for the tool-work thermocouple with the regression equation.

thermometer (Eurotherm, UK) measured the block's temperature. The corresponding voltage and temperature were recorded and plotted, revealing a linear relationship with the regression equation, as shown in Fig. 2(c), used to determine the chip-tool interface temperature from the thermocouple voltage.

Additionally, the thickness of the chips generated for each experimental run during turning was measured repeatedly using a digital vernier caliper (Mitutoyo Absolute Digimatic, 150 mm) with 0.01 mm of resolution to calculate the cutting ratio ($r_c$), which represents the chip thickness ratio before and after cutting. To ensure accuracy, multiple measurements were taken from different sections of the chip, and the process was repeated twice to confirm consistency. The material removal rate (MRR) was determined based on the depth of cut, feed rate, and cutting speed used in each experimental trial.

Surface roughness ($R_a$) was measured after each experimental run using a Talysurf roughness tester (Surtronic 3+, Rank Taylor Hobson Limited), with a commonly used cut-off length of 0.8 mm and a total evaluation length of 4 mm. Measurements were taken three times at different, evenly spaced locations on the cylindrical machined surface. The average of these measurements was then calculated for each run.

The main cutting force component (F) was recorded using a sensitive yet robust 3-D dynamometer (KISTLER) connected to a data acquisition system for storage on a PC, depicted in Fig. 1(a). The dynamometer was calibrated before each experiment, and force measurements were repeated twice to ensure consistency.

Tool life ($T_L$) was evaluated based on ISO Standard 3685 for tool life [44]. The average value of the principal flank wear ($V_B$) is the criterion that contributes to increased temperatures and cutting forces and can lead to machining vibrations over time. The cutting insert was periodically withdrawn at regular intervals during machining, and the principal feature $V_B$ was measured with an optical microscope (Carl Zeiss, Germany) equipped with a precision micrometer of least count 1 μm. The study continued until the value of $V_B$ exceeded 300 μm. At the end of machining and after significant wear, each tool's wear patterns and extent were examined with an SEM (Philips XL 30, Japan).

To improve measurement reliability in experiments, maintain stable environmental conditions (e.g., temperature and humidity) to avoid fluctuations affecting measurements. Regularly check and adjust MQL system parameters (pressure, flow rate) to ensure consistent cutting fluid application. Additionally, utilizing digital measuring instruments with high resolution and accuracy can further enhance reliability.

### 2.3. Machining parameters and responses

The Taguchi method utilizes an orthogonal array design to optimize processes where multiple control factors directly impact the desired output. To optimize parameters, a Taguchi $L_{18}$ (2^1, 3^2) mixed-level orthogonal array design was generated using Minitab19 software, considering the quantity and levels of input parameters involved. Table 2 displays the different levels of variable input parameters employed in the experiments. Based on previous studies on turning medium carbon steel [44–47], considering the lathe machine's power and capability and the tool manufacturer's recommendations, the feasible range of cutting parameters for the given cutting tool-workpiece system was selected. The orthogonal array ensures a balanced set of experiments incorporating multiple control parameters concurrently. The signal-to-noise (S/N) ratio represents a logarithmic function of the desired output, is used as the objective function for optimization. For beneficial criteria responses, the larger-the-better S/N ratio is used to maximize the respective responses. For non-beneficial criteria responses, the smaller-the-better S/N ratio is used to minimize the respective responses, ensuring optimal machinability.

The experimentation phase is complete with all 18 runs conducted, and data on multiple responses have been gathered for each trial. Table 3 details the experimental setting and the corresponding machining outcomes analyzed in this study.

## 3. Methodology

The study focuses on finding optimal machining parameters using diverse optimization techniques that address multiple conflicting responses concurrently. While the Taguchi method excels in optimizing process parameters with a single objective, it is complemented by methods like COPRAS, TOPSIS, MOORA, GRA, and CoCoSo for multi-response optimization. This research employs the Entropy method to determine the relative importance of each response variable. The detailed optimization steps are briefly discussed below.

### 3.1. Entropy method for weight determination

The entropy method determines how important each response is when optimizing with multiple objectives. This approach to weight determination is grounded in the principle that features exhibiting the greatest diversity in output parameters significantly impact those parameters. The Entropy method involves the following steps [48]:

**Table 2**
Levels of machining parameters.

| Machining parameters | Level 1 | Level 2 | Level 3 |
|---|---|---|---|
| Cooling Environment | Dry | MQL | |
| Cutting speed (m/min) | 137 | 160 | 178 |
| Feed rate (mm/rev) | 0.14 | 0.18 | 0.22 |

**Table 3**
The Orthogonal Array $L_{18}$ (2^1, 3^2) based on the Taguchi method with respective machining responses.

| Run order | Cooling Environment | Cutting speed | Feed rate | Beneficial criteria | | | Non-beneficial criteria | | |
|---|---|---|---|---|---|---|---|---|---|
| | | | | MRR | $r_c$ | $T_L$ | T | F | $R_a$ |
| 1 | Dry | 137 | 0.14 | 28770 | 0.38 | 17 | 768 | 757 | 1.79 |
| 2 | Dry | 137 | 0.18 | 36990 | 0.4 | 13 | 781 | 808 | 1.99 |
| 3 | Dry | 137 | 0.22 | 45210 | 0.42 | 10 | 798 | 834 | 2.36 |
| 4 | Dry | 160 | 0.14 | 33600 | 0.4 | 12 | 789 | 743 | 1.7 |
| 5 | Dry | 160 | 0.18 | 43200 | 0.42 | 9 | 803 | 792 | 1.84 |
| 6 | Dry | 160 | 0.22 | 52800 | 0.45 | 8 | 819 | 817 | 2.28 |
| 7 | Dry | 178 | 0.14 | 37380 | 0.41 | 8 | 810 | 731 | 1.62 |
| 8 | Dry | 178 | 0.18 | 48060 | 0.43 | 7 | 825 | 778 | 1.72 |
| 9 | Dry | 178 | 0.22 | 58740 | 0.47 | 6 | 844 | 805 | 2.22 |
| 10 | MQL | 137 | 0.14 | 28770 | 0.43 | 34 | 694 | 679 | 1.46 |
| 11 | MQL | 137 | 0.18 | 36990 | 0.45 | 27 | 714 | 709 | 1.78 |
| 12 | MQL | 137 | 0.22 | 45210 | 0.49 | 22 | 732 | 743 | 2.29 |
| 13 | MQL | 160 | 0.14 | 33600 | 0.44 | 21 | 709 | 655 | 1.4 |
| 14 | MQL | 160 | 0.18 | 43200 | 0.47 | 19 | 730 | 680 | 1.72 |
| 15 | MQL | 160 | 0.22 | 52800 | 0.51 | 18 | 743 | 713 | 2.24 |
| 16 | MQL | 178 | 0.14 | 37380 | 0.46 | 19 | 725 | 635 | 1.36 |
| 17 | MQL | 178 | 0.18 | 48060 | 0.5 | 16 | 745 | 650 | 1.67 |
| 18 | MQL | 178 | 0.22 | 58740 | 0.52 | 14 | 755 | 678 | 2.18 |

Step 1: Establish the decision matrix, incorporating the responses (n) from the experimental design for m alternatives. Here, $x_{ij}$ represents the element of the decision matrix corresponding to the ith alternative and the jth response.

$$X = \begin{bmatrix} x_{11} & x_{12} & \cdots & x_{1n} \\ x_{21} & x_{22} & \cdots & x_{2n} \\ \cdots & \cdots & \cdots & \cdots \\ x_{m1} & x_{m2} & \cdots & x_{mn} \end{bmatrix} \text{ Where, } i = 1, 2, 3, \ldots\ldots, m;\ j = 1, 2, 3, \ldots\ldots, n \tag{1}$$

Step 2: Normalize the decision matrix using Equation (2).

$$p_{ij} = \frac{x_{ij}}{\sum_{i=1}^{m} x_{ij}} \tag{2}$$

Step 3: Compute Entropy measure of the outcomes by Equation (3).

$$E_j = -k \sum_{i=1}^{m} p_{ij} \ln\left(p_{ij}\right) \tag{3}$$

where, $k = -1/\ln(m)$.

Step 4: Determine the objective weights of the responses according to Equation (4).

$$Wj = \frac{1 - E_j}{\sum_{j=1}^{n} \left(1 - E_j\right)} \tag{4}$$

### 3.2. Complex Proportional Assessment (COPRAS) method

The COPRAS method operates similarly to the Simple Additive Weighting (SAW) method. SAW is one of the simplest and most widely accepted MCDM methods. It evaluates both maximizing and minimizing index values, considering the effects of these indexes on the assessment of results separately. The COPRAS method incorporates maximizing (benefit) and minimizing (non-benefit) criteria in the decision matrix, standardizing the data to facilitate comparisons across various measurement units. Below are the essential steps of the COPRAS method [49]:

Step 1: Normalize the decision matrix according to Equation (5).

$$r_{ij} = \frac{x_{ij}}{\sum_{i=1}^{m} x_{ij}} \ (i = 1, 2, 3, \ldots., m;\ j = 1, 2, 3, \ldots.., n) \tag{5}$$

Step 2: Compute the weight-normalized matrix as follows.

$$y_{+ij} = r_{ij} \times w_j \tag{6}$$

Step 3: Compute the sums of weight-normalized scores for both benefit (maximizing) and non-benefit (minimizing) criteria as

follows.

$$S_{+i} = \sum_{j=1}^{n} y_{+ij}$$
$$S_{-i} = \sum_{j=1}^{n} y_{-ij} \quad (7)$$

In the above equation, $y_{+ij}$ pertains to maximizing criteria, while $y_{-ij}$ pertains to minimizing criteria. The alternatives are characterized by benefit (maximizing) criteria $S_{+i}$ and non-benefit (minimizing) criteria $S_{-i}$. Essentially, $S_{+i}$ and $S_{-i}$ indicate the extent to which the objectives are achieved by alternative i.

Step 4: The relative importance $Q_i$ of each alternative i is determined as follows.

$$Q_i = S_{+i} + \frac{S_{-\min} \sum_{i=1}^{m} S_{-i}}{S_{-i} \sum_{i=1}^{m} (S_{-\min}/S_{-i})} \quad (8)$$

The alternative with the highest $Q_i$ value ($Q_{max}$) is considered the best.

Step 5: Calculate the level of performance ($U_i$) for each alternative i as follows.

$$U_i = \frac{Q_i}{Q_{max}} \times 100\% \quad (9)$$

The utility degree is calculated by comparing each evaluated alternative to the most effective one, $Q_{max}$ (the highest relative importance score). The optimal alternative is represented by the highest degree of utility, $U_i$, which equals 100 %.

### 3.3. Technique for Order Preference by Similarity to Ideal Solution (TOPSIS) method

The TOPSIS is a modern method used to determine the optimal process conditions from the proposed experimental design. It efficiently identifies both the most favorable (maximum) and least favorable (minimum) process conditions. This method calculates the closeness coefficient, which measures how close each feasible solution is to the ideal solution, ensuring that the selected parameter is nearest to the best solution and furthest from the worst solution. Here are the outlined steps of the TOPSIS method [50]:

Step 1: Normalize the decision matrix using Equation (10).

$$r_{ij} = \frac{x_{ij}}{\sqrt{\sum_{i=1}^{m} x_{ij}^2}} \ (i = 1, 2, 3, \ldots m;\ j = 1, 2, 3, \ldots . n) \quad (10)$$

Step 2: Compute the weighted normalized matrix according to Equation (11).

$$V_{ij} = r_{ij} \times w_j \quad (11)$$

where, $w_j$ indicates the weight of each response j.

Step 3: Compute the ideal solution from the weighted decision matrix using Equation (12). The ideal solutions consist of both the positive (best) ideal solution ($V^+$) and negative (worst) solution ($V^-$) for each attribute.

$$V^+ = \left\{ \left( \mathrm{Max}(V_{ij}) \,|\, j \in J \right), \left( \mathrm{Min}(V_{ij}) \,|\, j \in J' \right) \right\}$$
$$V^- = \left\{ \left( \mathrm{Min}(V_{ij}) \,|\, j \in J \right), \left( \mathrm{Max}(V_{ij}) \,|\, j \in J' \right) | i = 1, 2 \quad m \right\} \quad (12)$$

Where J represents beneficial criteria and J′ denotes non-beneficial criteria.

Step 4: Measure the separation for each solution, represented as the positive (best) ideal solution ($D_i^+$) and negative (worst) solution ($D_i^-$) as follows.

$$D_i^+ = \sqrt{\sum_{j=1}^{n} \left( V_{ij} - V_j^+ \right)^2}$$
$$D_i^- = \sqrt{\sum_{j=1}^{n} \left( V_{ij} - V_j^- \right)^2} \quad (13)$$

Step 5: Calculate the closeness coefficient of each alternative ($C_i$) using Equation (14).

$$C_i = \frac{D_i^-}{D_i^- + D_i^+} \quad (14)$$

Sort the values in ascending order according to the closeness coefficient to find the best solution.

### 3.4. Multi-Objective Optimization Ratio Analysis (MOORA) method

The MOORA method is regarded as an objective (non-subjective) approach. It simultaneously evaluates desirable and undesirable criteria to choose the best alternative from various options. The MOORA method comprises the subsequent steps [51]:

Step 1: Create a ratio system by standardizing the data from the decision matrix. The normalized value can be computed using the following equation.

$$n_{ij} = \frac{x_{ij}}{\sqrt{\sum_{i=1}^{m} x_{ij}^2}} \ (i = 1, 2, 3, \ldots, m;\ j = 1, 2, 3, \ldots, n) \tag{15}$$

Step 2: Compute the weighted normalized decision matrix according to Equation (16).

$$N_{ij} = n_{ij} \times w_j \tag{16}$$

Step 3: Calculate the performance value (an overall assessment value of the performance measures) of each alternative as follows.

$$Y_i = \sum_{j=1}^{g} N_{ij} - \sum_{j=g+1}^{n} N_{ij} \tag{17}$$

where, g represents the number of responses categorized under the Larger-is-better criterion, (n-g) signifies the number of responses categorized under the Lower-is-better criterion, and $Y_i$ denotes the overall assessment value of the ith alternative relative to all alternatives. The $Y_i$ values are arranged in descending order, where the highest value signifies the optimal alternative and the lowest value signifies the least favorable one.

### 3.5. Grey Relational Analysis (GRA) method

The Grey Relational Analysis method is a specialized and widely adopted tool for investigating uncertainties in available data and assessing the effectiveness of unknown methods. Below are the three computational stages of GRA [52]:

Step 1: In normalization or data pre-processing, responses are converted into dimensionless values starting from 0 to 1, depending on whether the situation deems "smaller the better" or "larger the better." The responses are normalized according to the "smaller the better" and "larger the better" objectives, utilizing the following equations.

For, smaller the better:

$$y_i(k) = \frac{\max x_i(k) - x_i(k)}{\max x_i(k) - \min x_i(k)} \tag{18}$$

For, larger the better:

$$y_i(k) = \frac{x_i(k) - \min x_i(k)}{\max x_i(k) - \min x_i(k)} \tag{19}$$

Where $y_i(k)$ is the value after the grey relational generation, and $\min x_i(k)$ and $\max x_i(k)$ are the smallest value and largest values of $x_i(k)$ for the kth performance respectively.

Step 2: Calculating the Grey Relational Coefficient (GRC) for each experimental run using the equation provided below.

$$GRC = w_i(k) = \frac{\Delta min + p.\Delta max}{\Delta O_i(k) + p.\Delta max} \tag{20}$$

where $w_i$ (k) denotes the GRC value of each response for each experimental run i, p is the distinguishing coefficient, typically assumed to be 0.5 [52].

$\Delta O_i$ (k) = $\left\| y_o(k) - y_i(k) \right\|$ is the difference of the absolute value between $y_o(k)$ and $y_i(k)$.

$\Delta max = \forall$ j max $\in$ i$\forall$k max$\left\| y_o(k) - y_j(k) \right\|$ = the largest value of $\Delta O_i$ (k)

$\Delta min = \forall$ j min $\in$ i$\forall$k min$\left\| y_o(k) - y_j(k) \right\|$ = the smallest value of $\Delta O_i$ (k)

Step 3: Calculate the Grey Relational Grade (GRG) by multiplying the relative weight value ($w_k$) by the computed GRC, as described below.

$$GRG = \sum_{k=1}^{n} w_k \times w_i(k) \tag{21}$$

Arrange the GRG in ascending order to identify the optimal parameters. A higher GRG indicates the best-designed process, identifying the corresponding conditions as optimal.

### 3.6. Combined Compromised Solution (CoCoSo) method

The Combined Compromised Solution method is a recent addition to the field of Multiple Criteria Decision Making (MCDM). It efficiently categorizes or redirects alternatives by leveraging simple additive weighting and an exponentially weighted product model. The CoCoSo method follows the procedural steps [53]:

Step 1: Develop the initial decision matrix by formulating the corresponding matrix considering m alternatives (representing the number of experimental trials) and n criteria (representing the number of responses).

$$X = \begin{bmatrix} x_{11} & x_{12} & \cdots & x_{1n} \\ x_{21} & x_{22} & \cdots & x_{2n} \\ \cdots & \cdots & \cdots & \cdots \\ x_{m1} & x_{m2} & \cdots & x_{mn} \end{bmatrix} \text{ Where, } i = 1, 2, 3, \ldots\ldots, m;\ j = 1, 2, 3, \ldots\ldots, n \tag{22}$$

Step 2: Normalize the decision matrix based on the type of criterion under consideration using the following equations:
For benefit (Maximizing) criterion,

$$n_{ij} = \frac{x_{ij} - \min x_{ij}}{\max x_{ij} - \min x_{ij}} \tag{23}$$

For non-benefit (Minimizing) criterion,

$$n_{ij} = \frac{\max x_{ij} - x_{ij}}{\max x_{ij} - \min x_{ij}} \tag{24}$$

Step 3: Calculate the power of weighted (Pi) and sum of weighted (Si) comparability sequence scores for each alternative as follows:

$$P_i = \sum_{j=1}^{n} (n_{ij})^{w_j} \tag{25}$$

$$S_i = \sum_{j=1}^{n} (w_j \times n_{ij}) \tag{26}$$

Here, $w_j$ denotes the weight assigned to the jth criterion.
Step 4: Compute the appraisal scores for each alternative using three aggregation strategies as follows:

$$k_{ia} = \frac{P_i + S_i}{\sum_{i=1}^{m} (P_i + S_i)} \tag{27}$$

$$k_{ib} = \frac{P_i}{\min_i P_i} + \frac{S_i}{\min_i S_i} \tag{28}$$

$$k_{ic} = \frac{\lambda(S_i) + (1-\lambda)(P_i)}{\left(\lambda \max_i S_i + (1-\lambda) \max_i P_i\right)}, 0 \le \lambda \le 1 \tag{29}$$

Typically, the value of λ is set to 0.5 [53].
Step 5: Determine the value of the final appraisal score $k_i$. The ranking of alternatives is determined by the $k_i$ value, calculated using

**Table 4**
Decision matrix normalization.

| Run order | MRR | $r_c$ | $T_L$ | T | F | $R_a$ |
|---|---|---|---|---|---|---|
| 1 | 0.037388 | 0.047205 | 0.060714 | 0.055717 | 0.057318 | 0.053242 |
| 2 | 0.04807 | 0.049689 | 0.046429 | 0.05666 | 0.06118 | 0.059191 |
| 3 | 0.058752 | 0.052174 | 0.035714 | 0.057893 | 0.063148 | 0.070196 |
| 4 | 0.043665 | 0.049689 | 0.042857 | 0.05724 | 0.056258 | 0.050565 |
| 5 | 0.05614 | 0.052174 | 0.032143 | 0.058256 | 0.059968 | 0.054729 |
| 6 | 0.068616 | 0.055901 | 0.028571 | 0.059417 | 0.061861 | 0.067817 |
| 7 | 0.048577 | 0.050932 | 0.028571 | 0.058764 | 0.055349 | 0.048186 |
| 8 | 0.062456 | 0.053416 | 0.025 | 0.059852 | 0.058908 | 0.05116 |
| 9 | 0.076335 | 0.058385 | 0.021429 | 0.06123 | 0.060953 | 0.066032 |
| 10 | 0.037388 | 0.053416 | 0.121429 | 0.050348 | 0.051412 | 0.043427 |
| 11 | 0.04807 | 0.055901 | 0.096429 | 0.051799 | 0.053684 | 0.052945 |
| 12 | 0.058752 | 0.06087 | 0.078571 | 0.053105 | 0.056258 | 0.068114 |
| 13 | 0.043665 | 0.054658 | 0.075 | 0.051436 | 0.049595 | 0.041642 |
| 14 | 0.05614 | 0.058385 | 0.067857 | 0.05296 | 0.051488 | 0.05116 |
| 15 | 0.068616 | 0.063354 | 0.064286 | 0.053903 | 0.053987 | 0.066627 |
| 16 | 0.048577 | 0.057143 | 0.067857 | 0.052597 | 0.048081 | 0.040452 |
| 17 | 0.062456 | 0.062112 | 0.057143 | 0.054048 | 0.049216 | 0.049673 |
| 18 | 0.076335 | 0.064596 | 0.05 | 0.054774 | 0.051336 | 0.064842 |

the following equation.

$$k_i = (k_{ia} \times k_{ib} \times k_{ic})^{1/3} + \frac{1}{3}(k_{ia} + k_{ib} + k_{ic}) \quad (30)$$

The alternative with the highest $k_i$ is considered desirable and identified as the optimal solution.

## 4. Results, analysis and discussion

Five different MCDM approaches, encompassing COPRAS, TOPSIS, MOORA, GRA, and CoCoSo, are integrated with the Taguchi method in this study to optimize multiple responses for enhancing machinability. The weights for each response are determined using the Entropy method to support all MCDM techniques. The statistical software Minitab 19 is employed to analyze and assess the effects of process parameters, including feed rate, cutting speed, and cooling environment, on each specific MCDM method. SEM (Scanning electron microscopy) coupled with EDX (Energy-dispersive X-ray) analysis is conducted on the carbide insert under both cooling environments to gain a comprehensive understanding of how these environments impact tool wear and lifespan.

### 4.1. Weight calculation using the entropy method

The weight of each machining response was determined using the standard Entropy method, illustrated in Tables 4–6. The resulting weights for all machining responses, derived via the Entropy method, are displayed in Table 6. It is observed that the importance of all machining responses is comparable. These response weights have been subsequently applied in various MCDM techniques.

### 4.2. MCDM using COPRAS method

Multi-criteria decision-making with the COPRAS method was performed according to Equations (5)–(9), as outlined in the standard COPRAS method. Table 7 presents the relative importance ($Q_i$) and performance level ($U_i$) of alternatives. It can be found that the optimal alternative is run order 10, which has a feed rate of 0.14 mm/rev, a cutting speed of 137 m/min, and a cooling environment of MQL.

Fig. 3 displays the main effect plot representing the mean performance levels (Ui). It indicates a significant increase in performance level from Level 1 (Dry) to Level 2 (MQL), underscoring the substantial impact of the cooling environment. Performance peaks at the lowest cutting speed (Level 1) and slightly decreases at higher speeds. Similarly, performance is highest at the lowest feed rate (Level 1) and decreases with higher rates. Therefore, the cooling environment emerges as the most critical factor, suggesting that maintaining lower cutting speeds and feed rates can enhance performance in the COPRAS method. Table 8 ranks the impact of process parameters on the COPRAS index according to their delta values. The delta value, which measures the effect size by calculating the difference between the highest and lowest characteristic average for each parameter, indicates the degree of influence. The highest delta value for the cooling environment signifies its highest impact on the COPRAS index, subsequently by feed rate and cutting speed. The rankings in the response table quickly identify the most significant factors.

### 4.3. MCDM using TOPSIS method

The TOPSIS method was conducted following Equations (10)–(14), as outlined in the standard TOPSIS methodology. The separation and closeness coefficient values for each alternative are shown in Table 9. The analysis indicates that the optimal alternative is run order 10, which features a feed rate of 0.14 mm/rev, a cutting speed of 137 m/min, and a cooling environment of MQL.

Fig. 4 depicts the main effect plot illustrating the means of the closeness coefficient value (Ci). It is found that the best levels for achieving the highest performance are the cooling environment at Level 2 (MQL), the cutting speed at the lowest level (137 m/min), and the feed rate at the first level (0.14 mm/rev). Table 10 indicates that the cooling environment significantly affects the TOPSIS index, followed by cutting speed and feed rate.

### 4.4. MCDM using MOORA method

The MOORA method was carried out according to Equations (15)–(17), as described in the standard MOORA methodology. The performance value for each alternative (an overall assessment of the performance measures) is presented in Table 11. The result reveals that the optimal alternative is run order 10, characterized by a feed rate of 0.14 mm/rev, a cutting speed of 137 m/min, and a cooling environment of MQL.

Fig. 5 shows the main effect plot for means of the performance value (Yi). It reveals that the best levels for achieving the highest performance are the cooling environment at Level 2 (MQL), the cutting speed at the lowest level (137 m/min), and the feed rate at the

**Table 5**
Compute Entropy measure ($E_j$) of the responses.

| | MRR | $r_c$ | $T_L$ | T | F | $R_a$ |
|---|---|---|---|---|---|---|
| $E_j$ | −0.9923 | −0.99868 | −0.9637 | −0.99945 | −0.99881 | −0.99504 |

**Table 6**
Determine the objective weights of the responses.

| Machining response | Objective weight, $W_j = \frac{1 - E_j}{\sum_{j=1}^{n}(1 - E_j)}$ |
|---|---|
| MRR | 0.166747841 |
| $r_c$ | 0.167282093 |
| $T_L$ | 0.164354012 |
| T | 0.167346085 |
| F | 0.167292719 |
| $R_a$ | 0.166977251 |

**Table 7**
The relative importance ($Q_i$) and performance level ($U_i$) of each alternative.

| Run order | $Q_i$ | $U_i$ |
|---|---|---|
| 1 | 0.051813463 | 77.50234806 |
| 2 | 0.049980371 | 74.76041751 |
| 3 | 0.048484705 | 72.5232061 |
| 4 | 0.050713839 | 75.85753455 |
| 5 | 0.050006124 | 74.79893782 |
| 6 | 0.049851451 | 74.56757908 |
| 7 | 0.04969739 | 74.33713472 |
| 8 | 0.050567652 | 75.63886935 |
| 9 | 0.050493683 | 75.52822656 |
| 10 | 0.066854056 | 100 |
| 11 | 0.062292584 | 93.1769707 |
| 12 | 0.058851744 | 88.03017706 |
| 13 | 0.06103617 | 91.29763256 |
| 14 | 0.059884515 | 89.57499189 |
| 15 | 0.05900438 | 88.25848922 |
| 16 | 0.061449545 | 91.91595608 |
| 17 | 0.060316711 | 90.22146836 |
| 18 | 0.058701617 | 87.80561826 |

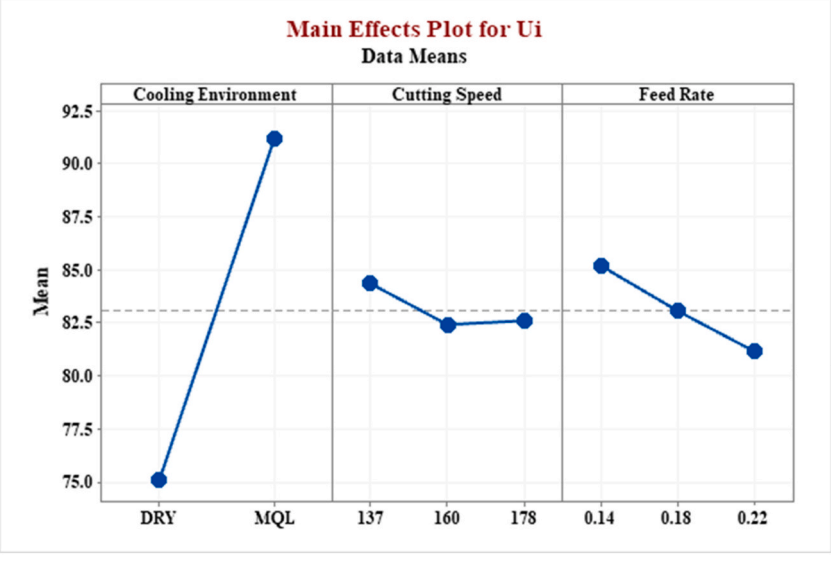


**Fig. 3.** Main effect plot for means of level of performance (Ui).

**Table 8**
Response table for means of COPRAS index.

| Level | Cooling Environment | Cutting Speed | Feed Rate |
|---|---|---|---|
| 1 | 75.06 | **84.33**[a] | **85.15**[a] |
| 2 | **91.14**[a] | 82.39 | 83.03 |
| 3 | | 82.57 | 81.12 |
| Delta | 16.09 | 1.94 | 4.03 |
| Rank | 1 | 3 | 2 |

[a] Indicates optimal levels of process parameters for the COPRAS index.

**Table 9**
Determine the separation as the positive (best) ideal solution ($D_i^+$) and negative (worst) solution ($D_i^-$) using the Euclidean distance and the closeness coefficient value of each alternative ($C_i$).

| Run order | $D_i^+$ | $D_i^-$ | $C_i$ |
|---|---|---|---|
| 1 | 0.049868118 | 0.028084879 | 0.360279651 |
| 2 | 0.054927265 | 0.019463823 | 0.261641871 |
| 3 | 0.061094936 | 0.017836181 | 0.225971481 |
| 4 | 0.056521276 | 0.02061776 | 0.267280493 |
| 5 | 0.060474273 | 0.018785687 | 0.237013583 |
| 6 | 0.063330756 | 0.023036506 | 0.266727294 |
| 7 | 0.063217674 | 0.018898965 | 0.230147814 |
| 8 | 0.063461968 | 0.02263286 | 0.26288292 |
| 9 | 0.066885772 | 0.028287491 | 0.297220989 |
| 10 | 0.028269755 | 0.067008301 | 0.703292063 |
| 11 | 0.027623547 | 0.050726004 | 0.647431964 |
| 12 | 0.036042547 | 0.040924859 | 0.531716753 |
| 13 | 0.037734839 | 0.04159878 | 0.524352485 |
| 14 | 0.03775926 | 0.037025261 | 0.495092576 |
| 15 | 0.041123785 | 0.037499127 | 0.476949099 |
| 16 | 0.039311465 | 0.039404953 | 0.500593831 |
| 17 | 0.042361086 | 0.035355578 | 0.454929179 |
| 18 | 0.048399585 | 0.036175918 | 0.427735178 |

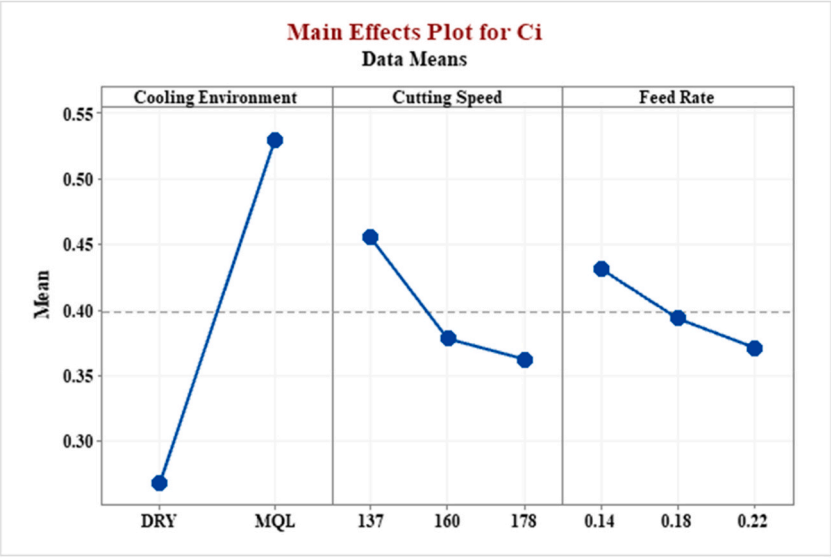


**Fig. 4.** Main effect plot for means of closeness coefficient value (Ci).

**Table 10**
Response table for means of TOPSIS index.

| Level | Cooling Environment | Cutting Speed | Feed Rate |
|---|---|---|---|
| 1 | 0.2677 | **0.4551**[a] | **0.4310**[a] |
| 2 | **0.5291**[a] | 0.3779 | 0.3932 |
| 3 | | 0.3623 | 0.3711 |
| Delta | 0.2614 | 0.0928 | 0.0599 |
| Rank | 1 | 2 | 3 |

[a] Indicates optimal levels of process parameters for the TOPSIS index.

**Table 11**
Calculate the performance value, an overall assessment value of the performance measures ($Y_i$) of each alternative.

| Run order | $Y_i$ |
|---|---|
| 1 | −0.01961 |
| 2 | −0.02704 |
| 3 | −0.03461 |
| 4 | −0.02325 |
| 5 | −0.02588 |
| 6 | −0.02817 |
| 7 | −0.02677 |
| 8 | −0.02303 |
| 9 | −0.02498 |
| 10 | 0.037986 |
| 11 | 0.022056 |
| 12 | 0.008337 |
| 13 | 0.015632 |
| 14 | 0.013322 |
| 15 | 0.009974 |
| 16 | 0.017355 |
| 17 | 0.015433 |
| 18 | 0.009673 |

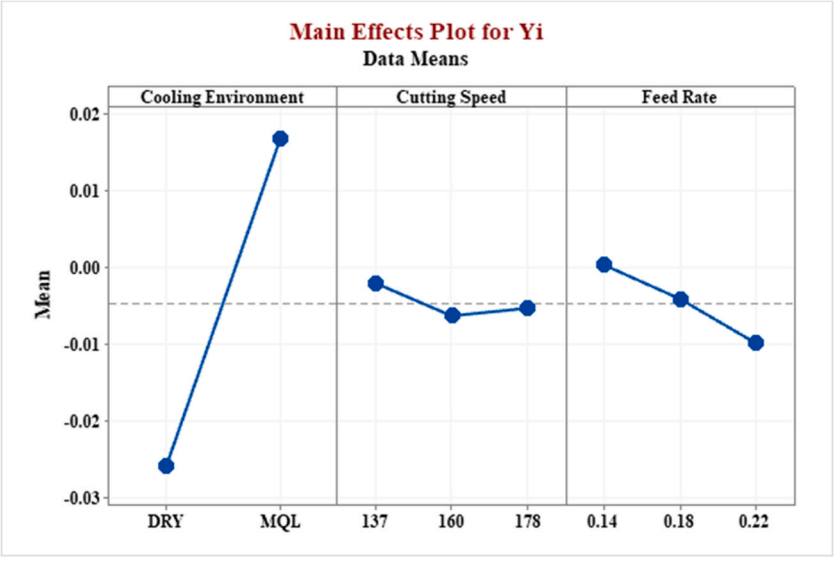


**Fig. 5.** Main effect plot for means of performance value (Yi).

lowest level (0.14 mm/rev). Table 12 indicates that the cooling environment is the dominant factor affecting the MOORA index, with feed rate being the second most crucial factor and cutting speed having a lesser effect.

**Table 12**
Response table for means of MOORA index.

| Level | Cooling Environment | Cutting Speed | Feed Rate |
|---|---|---|---|
| 1 | −0.025929 | **−0.002147**[a] | **0.000223**[a] |
| 2 | **0.016641**[a] | −0.006396 | −0.004191 |
| 3 | | −0.005388 | −0.009964 |
| Delta | 0.042570 | 0.004249 | 0.010187 |
| Rank | 1 | 3 | 2 |

[a] Indicates optimal levels of process parameters for the MOORA index.

**Table 13**
Determine Grey Relational Coefficient (GRC) and Grey Relational Grade (GRG) of each experimental run.

| Run order | MRR | $r_c$ | $T_L$ | T | F | $R_a$ | GRG |
|---|---|---|---|---|---|---|---|
| 1 | 0.333333 | 0.333333 | 0.451613 | 0.503356 | 0.44921 | 0.537634 | 0.434725 |
| 2 | 0.407922 | 0.368421 | 0.4 | 0.462963 | 0.365138 | 0.442478 | 0.407836 |
| 3 | 0.525513 | 0.411765 | 0.368421 | 0.418994 | 0.333333 | 0.333333 | 0.398601 |
| 4 | 0.373458 | 0.368421 | 0.388889 | 0.441176 | 0.479518 | 0.595238 | 0.441259 |
| 5 | 0.490909 | 0.411765 | 0.358974 | 0.407609 | 0.387914 | 0.510204 | 0.428037 |
| 6 | 0.716129 | 0.5 | 0.35 | 0.375 | 0.353464 | 0.352113 | 0.441259 |
| 7 | 0.412299 | 0.388889 | 0.35 | 0.39267 | 0.508951 | 0.657895 | 0.452037 |
| 8 | 0.583869 | 0.4375 | 0.341463 | 0.364078 | 0.410309 | 0.581395 | 0.453314 |
| 9 | 1 | 0.583333 | 0.333333 | 0.333333 | 0.369202 | 0.367647 | 0.498049 |
| 10 | 0.333333 | 0.4375 | 1 | 1 | 0.69338 | 0.833333 | 0.715614 |
| 11 | 0.407922 | 0.5 | 0.666667 | 0.789474 | 0.573487 | 0.543478 | 0.580034 |
| 12 | 0.525513 | 0.7 | 0.538462 | 0.663717 | 0.479518 | 0.34965 | 0.542898 |
| 13 | 0.373458 | 0.466667 | 0.518519 | 0.833333 | 0.832636 | 0.925926 | 0.658916 |
| 14 | 0.490909 | 0.583333 | 0.482759 | 0.675676 | 0.688581 | 0.581395 | 0.584129 |
| 15 | 0.716129 | 0.875 | 0.466667 | 0.604839 | 0.560563 | 0.362319 | 0.597978 |
| 16 | 0.412299 | 0.538462 | 0.482759 | 0.707547 | 1 | 1 | 0.690843 |
| 17 | 0.583869 | 0.777778 | 0.4375 | 0.595238 | 0.868996 | 0.617284 | 0.647432 |
| 18 | 1 | 1 | 0.411765 | 0.551471 | 0.698246 | 0.378788 | 0.674052 |

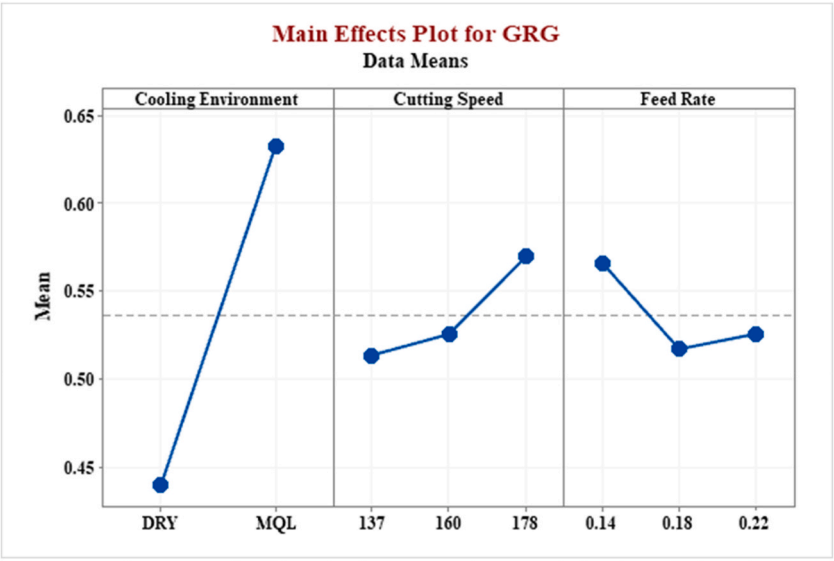


**Fig. 6.** Main effect plot for means of Grey Relational Grade (GRG).

### 4.5. MCDM using GRA method

The GRA method was performed according to Equations (18)–(21), as outlined in the standard GRA methodology. The grey relational coefficient (GRC) and grey relational grade (GRG) for each alternative are shown in Table 13. The results indicate that the optimal alternative is run order 10, which features a feed rate of 0.14 mm/rev, a cutting speed of 137 m/min, and a cooling environment of MQL.

**Table 14**
Response table for means of GRA index.

| Level | Cooling Environment | Cutting Speed | Feed Rate |
|---|---|---|---|
| 1 | 0.4395 | 0.5133 | **0.5656**[a] |
| 2 | **0.6324**[a] | 0.5253 | 0.5168 |
| 3 | | **0.5693**[a] | 0.5255 |
| Delta | 0.1930 | 0.0560 | 0.0488 |
| Rank | 1 | 2 | 3 |

[a] Indicates optimal levels of process parameters for the GRA index.

**Table 15**
Compute the appraisal scores for each alternative using three aggregation strategies and the value of the final appraisal score ($K_i$).

| Run order | $K_{ia}$ | $K_{ib}$ | $K_{ic}$ | $K_i$ |
|---|---|---|---|---|
| 1 | 0.039912 | 2.521727 | 0.607051 | 1.45009 |
| 2 | 0.05233 | 2.691545 | 0.795927 | 1.662113 |
| 3 | 0.036296 | 2 | 0.552049 | 1.204988 |
| 4 | 0.054559 | 3.05996 | 0.829827 | 1.832217 |
| 5 | 0.054026 | 2.954889 | 0.821724 | 1.784988 |
| 6 | 0.050599 | 2.727903 | 0.769593 | 1.656295 |
| 7 | 0.054325 | 3.094634 | 0.826266 | 1.84297 |
| 8 | 0.053684 | 3.095494 | 0.816523 | 1.835764 |
| 9 | 0.038582 | 2.538448 | 0.586819 | 1.440525 |
| 10 | 0.056956 | 4.605579 | 0.866284 | 2.45317 |
| 11 | 0.063314 | 4.476137 | 0.962995 | 2.482797 |
| 12 | 0.060327 | 4.084438 | 0.917555 | 2.296637 |
| 13 | 0.063832 | 4.702605 | 0.970877 | 2.57544 |
| 14 | 0.064359 | 4.629188 | 0.97888 | 2.553962 |
| 15 | 0.062363 | 4.423346 | 0.94853 | 2.451015 |
| 16 | 0.065285 | 4.914743 | 0.992967 | 2.67399 |
| 17 | 0.065747 | 4.941071 | 1 | 2.689709 |
| 18 | 0.063506 | 4.66456 | 0.965915 | 2.556948 |

Fig. 6 illustrates the main effect plot for the means of Grey Relational Grade (GRG). It indicates that the optimal conditions for achieving the highest performance are a Level 2 (MQL) cooling environment, the highest cutting speed (178 m/min), and the lowest feed rate (0.14 mm/rev). Table 14 shows that the cooling environment exerts the greatest influence on the GRA index, followed by cutting speed and feed rate.

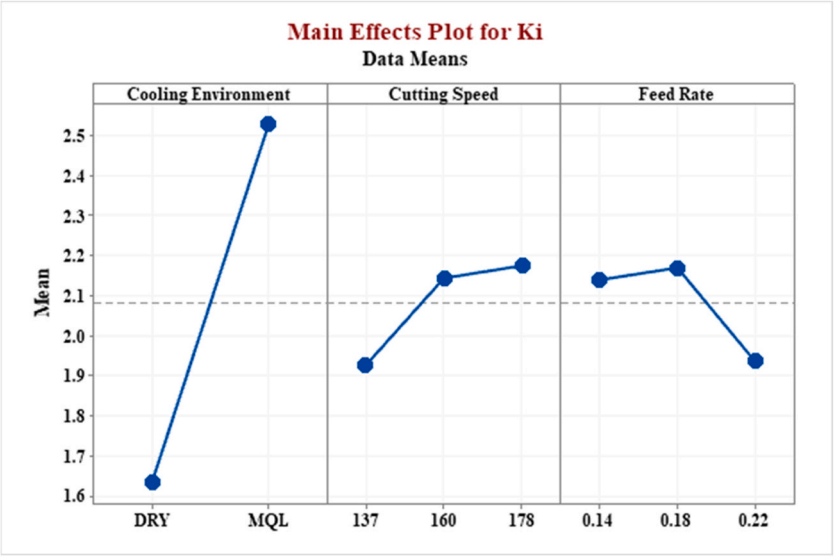


**Fig. 7.** Main effect plot for means of final appraisal score (Ki).

**Table 16**
Response table for means of CoCoSo index.

| Level | Cooling Environment | Cutting Speed | Feed Rate |
|---|---|---|---|
| 1 | 1.634 | 1.925 | 2.138 |
| 2 | **2.526**[a] | 2.142 | **2.168**[a] |
| 3 | | **2.173**[a] | 1.934 |
| Delta | 0.892 | 0.248 | 0.234 |
| Rank | 1 | 2 | 3 |

[a] Indicates optimal levels of process parameters for the CoCoSo index.

### 4.6. MCDM using CoCoSo method

The CoCoSo method was conducted following Equations (22)–(30), as detailed in the standard CoCoSo methodology. The appraisal scores for each alternative, calculated using three aggregation strategies, and the final appraisal score ($K_i$) are presented in Table 15. The results show that the optimal alternative is run order 17, characterized by a feed rate of 0.18 mm/rev, a cutting speed of 178 m/min, and a cooling environment of MQL.

Fig. 7 presents the main effect plot for means of the final appraisal score (Ki). It reveals that the best levels for achieving the highest performance are the cooling environment at Level 2 (MQL), the cutting speed at the highest level (178 m/min), and the feed rate at the second level (0.18 mm/rev). Table 16 indicates that the largest Delta (0.892) signifies the most significant impact of the cooling environment on the CoCoSo index, with cutting speed being the second most influential factor at a Delta of 0.248, while feed rate has the least impact.

### 4.7. Confirmation test

After identifying the optimal machining parameters through various MCDM techniques—such as CoCoSo, GRA, MOORA, TOPSIS, and COPRAS—a confirmation run was performed for each method to validate their predictions. These tests aimed to ensure that the chosen optimal parameters would result in the best possible machining performance, as predicted by each MCDM approach. The optimal parameter settings were swiftly determined using the response table and main effect plot for the means of the MCDM methods' indices. Subsequently, the predicted value of the method's index at the optimal parameter levels was calculated using the following equation [47,54].

$$\gamma = \gamma_m + \sum_{j=1}^{p} \left(\gamma_j - \gamma_m\right) \tag{31}$$

Where, $\gamma$ = Predicted outcome, $\gamma_m$ = Total mean of the outcome across all experimental runs, $\gamma_j$ = Mean of the outcome at the optimal level for each process parameter, and $p$ = Number of process parameters.

The experimental values of the MCDM methods' indices from the confirmation run, along with the predicted results, are presented in Table 17. The predicted values for CoCoSo and GRA closely match the experimental results, while the discrepancies are significantly higher for MOORA, followed by TOPSIS. The absolute percentage errors between the predicted and experimental results have been calculated and are also listed in Table 17. Specifically, the errors were found to be 5.573 % for the COPRAS Index ($U_i$), 12.076 % for the TOPSIS Index ($C_i$), 36.809 % for the MOORA Index ($Y_i$), 0.659 % for the GRA Index (GRG), and 0.647 % for the CoCoSo Index ($K_i$). The degree of agreement between the predicted and experimental results was analyzed to assess the reliability of each MCDM technique in optimizing the turning parameters for medium carbon steel. The analysis indicates that CoCoSo and GRA are more reliable than the other MCDM methods.

### 4.8. Comparison of different MCDM methods

The ranking outcomes of the MCDM methods used in this study are depicted in Fig. 8 to evaluate the outcomes of the MCDM method, indicating generally consistent results. However, the CoCoSo method exhibits divergence from the others. Consequently, Spearman's rank correlation coefficient [55] is employed to measure the degree of correlation between these methods. Spearman's rank correlation coefficient evaluates the strength of a monotonic association between two variables that have been ranked, similar to

**Table 17**
Results of the confirmation tests for each MCDM method at their optimal machining parameters.

| Outcomes | Experimental Result | Predicted Result | Absolute % Error |
|---|---|---|---|
| COPRAS Index ($U_i$) | 100 | 94.42681493 | 5.573 |
| TOPSIS Index ($C_i$) | 0.703292063 | 0.618361565 | 12.076 |
| MOORA Index ($Y_i$) | 0.037986 | 0.024003667 | 36.809 |
| GRA Index (GRG) | 0.690843 | 0.695396056 | 0.659 |
| CoCoSo Index ($K_i$) | 2.689709 | 2.707100944 | 0.647 |

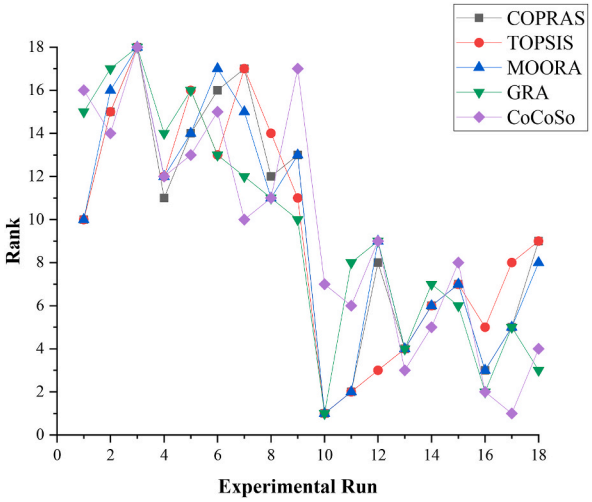


**Fig. 8.** Comparison of the five different MCDM methods.

**Table 18**
Spearman's rank correlation coefficient for five MCDM methods.

| Method | COPRAS | TOPSIS | MOORA | GRA | CoCoSo |
|---|---|---|---|---|---|
| COPRAS | 1 | | | | |
| TOPSIS | 0.93808 | 1 | | | |
| MOORA | 0.98968 | 0.909185 | 1 | | |
| GRA | 0.832817 | 0.79773 | 0.863777 | 1 | |
| CoCoSo | 0.789474 | 0.671827 | 0.820433 | 0.849329 | 1 |

how Pearson's correlation coefficient assesses linear relationships between variables. The correlation coefficients are calculated as per the following equation [56].

Spearman's Rank Correlation Coefficient:

$$r_s = 1 - \frac{6\sum d_i^2}{N(N^2-1)} \tag{32}$$

where, $d_i$ = Difference between ranks of two methods and $N$ = Number of trials or experimental runs.

The correlation results are shown in Table 18. Notably, the highest correlation coefficient, 0.98968, is between MOORA and COPRAS. The second highest, 0.93808, is between TOPSIS and COPRAS. The subsequent strongest correlation, with a coefficient of 0.909185, is between MOORA and TOPSIS. Furthermore, Spearman's rank correlation coefficients among these three methods should be thoroughly compared with previous studies. After reviewing several studies, it was found that Bandyopadhyay [57] reported a correlation coefficient of 0.9121 between MOORA and COPRAS in the selection of sewing robots, while Mousavi-Nasab et al. [58] found a coefficient of 0.964 in material selection problems. Bandyopadhyay [57] also identified a correlation coefficient of 0.8667 between TOPSIS and COPRAS for sewing robot selection. Sałabun et al. [59] observed a coefficient of 0.83 in numerical experiments, Więckowski et al. [60] reported 0.799 in laptop assessments, and Mousavi-Nasab et al. [58] reported 0.892 for material selection issues. Additionally, Moradian et al. [55] found a correlation coefficient of 0.9941 between MOORA and TOPSIS for material selection of a brake booster valve body, while Bandyopadhyay [57] reported 0.9636 in the context of sewing robot selection. Overall, Spearman's rank correlation coefficients among these three methods align reasonably well with previous studies. The discrepancies between our current findings and prior research might stem from application differences. Future research should focus on comparing the correlations of MCDM methods within similar contexts to ensure more accurate comparisons.

The observations presented in Table 19, gathered during this study's application of the MCDM methods, highlight their data normalization techniques and unique characteristics, providing a clear comparison.

### *4.9. Analysis of the impact of different cooling environments on tool wear and tool life*

The SEM was used to observe the wear patterns and extents on various surfaces of the carbide inserts after machining medium carbon steels over an extended period. This was done to assess how different cooling conditions influenced the wear of the inserts. SEM views depicting the principal and auxiliary flanks of worn SNMM carbide inserts used in machining medium carbon steel under both dry and MQL conditions are illustrated in Figs. 9 and 10, respectively.

**Table 19**
Comparison of different MCDM methods considering data normalization techniques and characteristics observed during their utilization in this study.

| MCDM Methods | Data Normalization Technique | Characteristic |
|---|---|---|
| COPRAS | Sum based linear normalization | This approach assesses the impact of maximizing and minimizing criteria independently. Its mathematical formulation resolves the issue of rank reversal and involves straightforward calculations. |
| TOPSIS | Vector normalization | The method's rationale and concept are easily understandable, with a straightforward mathematical form. |
| MOORA | Vector normalization | The method relies on a robust mathematical technique and involves simple calculations. |
| GRA | Max - Min linear normalization | Based on a robust mathematical framework, the method guarantees accuracy and dependability. It consistently delivers reliable outcomes while boasting a simple and comprehensible computational process. It efficiently employs available information, even if it is not necessarily independent. |
| CoCoSo | Max - Min linear normalization | The approach is exceptionally dependable in determining the optimal consensus score through its integrated framework. It aims to achieve a compromise that effectively balances conflicting objectives or criteria. Its transparency in decision-making empowers stakeholders to grasp the decision-making process. Its design enables the construction of a robust model, leading to more precise decision-making. |

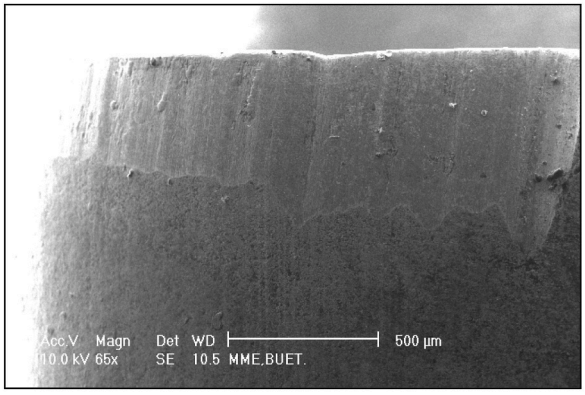


**(a) Dry machining, 15 min**

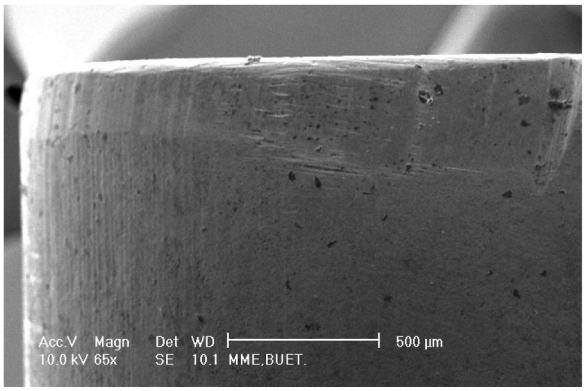


**(b) MQL machining, 15 min**

**Fig. 9.** SEM images showing the principal flank of worn SNMM carbide insert tip after machining medium carbon steel under (a) dry and (b) MQL conditions.

The SEM view in Fig. 9(a) shows significant wear, with clear signs of abrasion and potential adhesive wear mechanisms. The tool surface appears rough and uneven, indicating high wear rates. In contrast, the wear on the principal flank under MQL conditions in Fig. 9(b) is visibly reduced. The surface is smoother with fewer signs of severe abrasion, suggesting that MQL significantly mitigates wear compared to dry conditions. The auxiliary flank under dry conditions in Fig. 10(a) shows extensive wear, similar to the principal flank. The tool surface exhibits pronounced wear marks and potential thermal damage. Meanwhile, the auxiliary flank under MQL conditions in Fig. 10(b) shows reduced wear. The wear patterns are less pronounced, indicating that MQL helps to reduce both abrasive and thermal wear mechanisms.

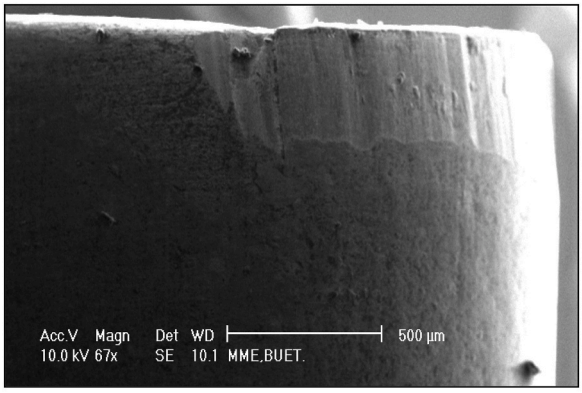


**(a) Dry machining, 15 min**

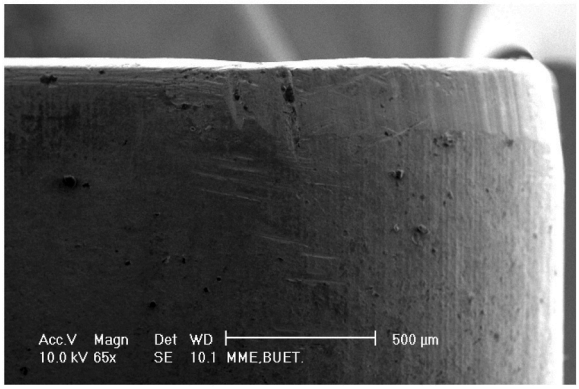


**(b) MQL machining, 15 min**

**Fig. 10.** SEM images showing the auxiliary flank of worn SNMM carbide insert tip after machining medium carbon steel under (a) dry and (b) MQL conditions.

Bar charts in Fig. 11 depict the comparative effectiveness of MQL versus dry conditions when machining medium carbon steel with SNMM carbide inserts across various speed and feed rate combinations. Fig. 11(a) shows that the tool life under dry conditions ranges from approximately 10 to 17 min at lower cutting velocities and feed rates. As cutting velocity increases, the tool life decreases, indicating that higher speeds exacerbate wear under dry conditions. Tool life under MQL conditions, as shown in Fig. 11(b), is significantly higher across all cutting velocities and feed rates compared to dry conditions. At similar cutting velocities and feed rates, the tool life ranges from approximately 14 to 34 min. The increased tool life under MQL conditions demonstrates the effectiveness of lubrication in reducing wear and extending tool life.

During the machinability study of hard-turning AISI 4140 steel using CC6050 tools under different cooling environments (dry and MQL) [61], long-term wear tests were conducted via straight turning at a feed rate of 0.12 mm/rev, a depth of cut of 0.15 mm, and a cutting speed of 120 m/min to assess tool life in different cooling conditions, revealing tool life of 32 min for dry cutting and 37 min for MQL. This improvement is attributed to the reduced friction between the chip and tool and between the workpiece and tool, which lowers local high temperatures and pressure at the tool's edge, thereby minimizing thermal impact. Swain et al. [62] performed turning of Ti-6Al-4V alloy using a CNMG 1020408 uncoated carbide tool at a depth of cut of 0.4 mm, a feed rate of 0.1 mm, and a cutting speed of 75 m/min to assess tool life under dry and MQL conditions. The tool life was 25 min in the dry environment and 95 min under MQL, indicating that MQL extended tool life by 280 % compared to dry cutting under the same parameters. Barari et al. [63] observed that the tool life of tungsten carbide significantly improved when turning 316L stainless steel under MQL compared to dry cutting, with nearly double the tool life recorded for MQL. This enhancement is due to the thermal gradient rapidly dissipating the heat generated in the cutting zone.

However, the current research findings on the tool life of SNMM carbide inserts are promising for turning medium carbon steel across the different speed and feed rate combinations examined.

Energy Dispersive X-ray (EDX) analysis was conducted on the carbide insert used under dry conditions, highlighting two specific points (Point-1 and Point-2) at an accelerating voltage of 20 kV and a magnification of 10,000. The analysis results are presented in Fig. 12. It is evident from the analysis that the white phase is tungsten carbide (WC), and the dark phase consists of tungsten, titanium,

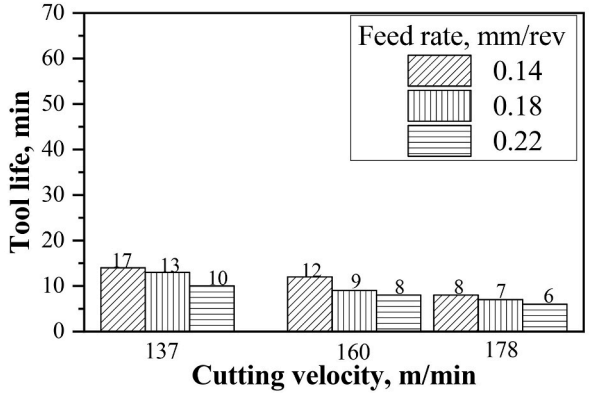


(a) Dry conditions

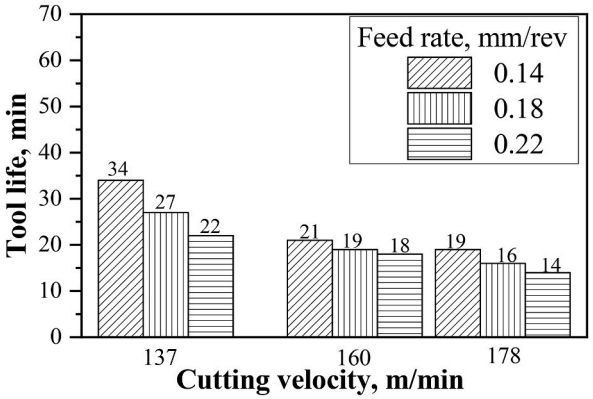


(b) MQL conditions

**Fig. 11.** Effect of (a) Dry and (b) MQL on tool life of SNMM carbide insert based on limiting average principal flank wear criteria $V_B = 300$ μm.

and tantalum carbide (WC-TiC-TaC) with cobalt as a binder. Additionally, EDX analysis was performed on the carbide inserts used in MQL conditions with two points (Point-1 and Point-2) at an accelerating voltage of 20 kV and a magnification of 25,000. The analysis result is shown in Fig. 13. The results indicate that the white phase is WC, and the dark phase is WC-TiC-TaC, with cobalt as a binder in both phases. The dimensions of the carbide particles within the inserts were estimated under both dry and MQL conditions.

Both cooling conditions feature similar phases, primarily tungsten carbide (WC) and tungsten titanium tantalum carbide (WC-TiC-TaC), with cobalt as a binder. Under dry conditions, the EDX analysis shows a higher concentration of tungsten in the primary WC phase. Under MQL conditions, cobalt is noticeable in both the primary and secondary phases, suggesting better distribution and potentially enhanced wear resistance due to the lubricating effect of cobalt. The presence of titanium and tantalum carbides in both conditions highlights these elements' role in enhancing the inserts' hardness and wear resistance. However, the higher cobalt content under MQL conditions may contribute to reduced wear, as evidenced by the smoother surfaces and fewer wear marks observed in the SEM images.

## 5. Conclusion

An uncoated carbide insert is used to evaluate the machinability of medium carbon steel in both dry and MQL cooling environments. Five different Taguchi-based Multi-Criteria Decision Making (MCDM) methods, namely CoCoSo, GRA, MOORA, TOPSIS, and COPRAS, are combined with the Entropy method to optimize multiple machining responses. This optimization aims to enhance machinability regarding material removal rate, surface roughness, main cutting force, cutting temperature, cutting ratio, and tool life to determine the optimal cutting parameters. The study leads to the following specific conclusions:

1. Across all MCDM methods (COPRAS, TOPSIS, MOORA, GRA, and CoCoSo), the main effect plots consistently demonstrate that the cooling environment is the most significant parameter. There is a clear trend that enhancing the cooling environment from Level 1 (Dry) to Level 2 (MQL) significantly improves performance. Cutting speed and feed rate show a negative trend with increasing levels for COPRAS, TOPSIS, and MOORA methods, indicating that lower cutting speeds and feed rates favor incremental benefits. While for GRA and CoCoSo methods, this trend is different for cutting speed.

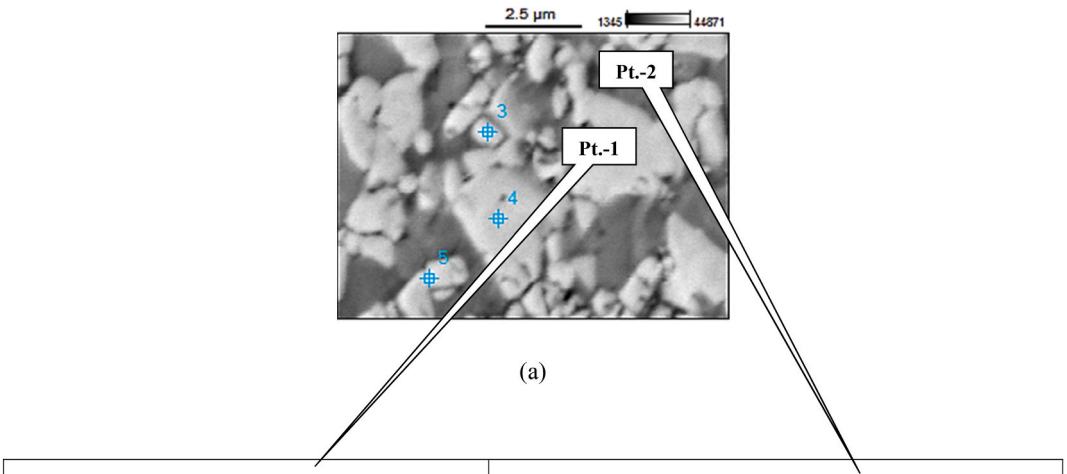


Weight %

| | C | Ti | Co | Ta | W |
|---|---|---|---|---|---|
| **Point-1** | 12.31 | | | | 87.69 |

(b)

Weight %

| | C | Ti | Co | Ta | W |
|---|---|---|---|---|---|
| **Point-2** | 10.70 | 19.20 | 2.94 | 27.35 | 39.81 |

(c)

**Fig. 12.** (a) SEM image of the SNMM carbide insert used in dry environment, highlighting different points (1 and 2) for phase identification [magnification ×10000], (b) EDX analysis at point-1, and (c) EDX analysis at point-2.

2. The cooling environment consistently emerges as the most influential process parameter across all MCDM methods (COPRAS, TOPSIS, MOORA, GRA, and CoCoSo) in response table analysis. This suggests that optimizing the cooling environment is critical for improving machinability. Although essential, cutting speed and feed rate have lesser impacts on all MCDM methods than the cooling environment, with cutting speed generally having a more significant influence than feed rate.
3. It can be concluded that the four MCDM methods—COPRAS, TOPSIS, MOORA, and GRA—yield the same optimal machining parameter setting: a feed rate of 0.14 mm/rev, a cutting speed of 137 m/min, and a cooling environment of MQL. In contrast, the CoCoSo method identifies a different optimal setting, with a feed rate of 0.18 mm/rev, a cutting speed of 178 m/min, and a cooling environment of MQL. When comparing the machining responses of the two optimal parameter settings, the setting for the four MCDM methods (run order 10) proves superior to that of the CoCoSo method (run order 17). Specifically, run order 10 yields a tool life of 34 min—more than double that of run order 17, which is 16 min, covering lower MRR. Additionally, run order 10 results in lower cutting temperatures, with other responses being comparable. Therefore, this study recommends the optimal machining parameter setting of a 0.14 mm/rev feed rate, a 137 m/min cutting speed, and using MQL as the cooling environment.
4. Based on the confirmation run, the CoCoSo and GRA methods demonstrate the highest reliability in predicting machining performance, as evidenced by their minimal discrepancies between predicted and experimental results. The absolute percentage errors are 5.573 % for the COPRAS Index (Ui), 12.076 % for the TOPSIS Index (Ci), 36.809 % for the MOORA Index (Yi), 0.659 % for the

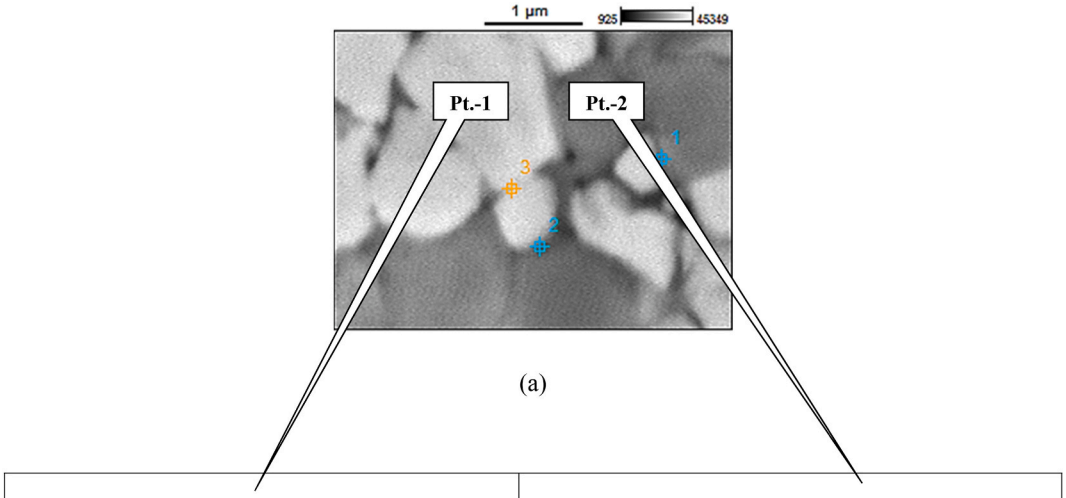


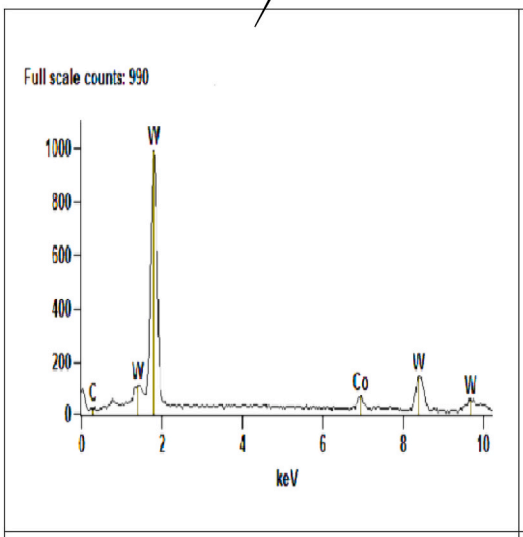


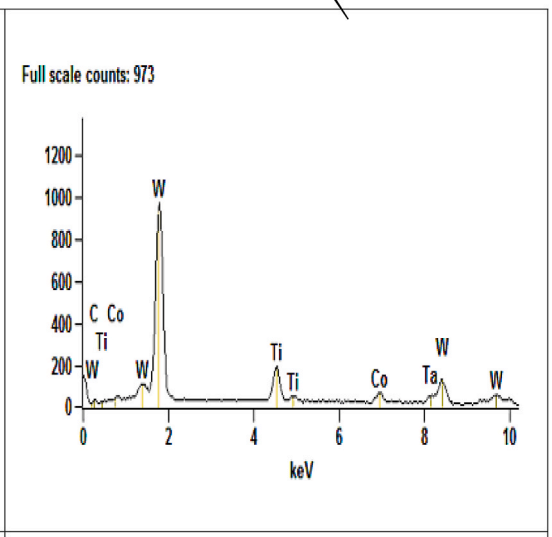


Weight %

| | C | Ti | Co | Ta | W |
|---|---|---|---|---|---|
| **Point-1** | 12.60 | | 5.76 | | 81.64 |

(b)

Weight %

| | C | Ti | Co | Ta | W |
|---|---|---|---|---|---|
| **Point-2** | 6.70 | 11.60 | 5.68 | 15.65 | 60.37 |

(c)

**Fig. 13.** (a) SEM image of the SNMM carbide insert used in the MQL environment, highlighting different points (1 and 2) for phase identification [magnification ×25000], (b) EDX analysis at point-1, and (c) EDX analysis at point-2.

GRA Index (GRG), and 0.647 % for the CoCoSo Index (Ki). The lower errors for CoCoSo, GRA, and COPRAS suggest that these methods are more effective in optimizing turning parameters for medium carbon steel than MOORA and TOPSIS.

5. The highest Spearman's rank correlation coefficient observed is between MOORA and COPRAS (0.98968), followed by TOPSIS and COPRAS (0.93808), and MOORA and TOPSIS (0.909185). Among these methods, COPRAS exhibits the lowest error (5.573 %) in predicting machining performance. Consequently, COPRAS could effectively replace MOORA and TOPSIS in similar decision-making scenarios. However, each MCDM method offers distinct advantages based on its normalization technique and inherent characteristics.
6. SEM images indicate that auxiliary flank and principal flank wear of the SNMM carbide inserts is significantly reduced under MQL conditions compared to dry machining. The smoother surfaces and fewer wear marks under MQL conditions suggest that lubrication effectively mitigates abrasive and adhesive wear mechanisms. Additionally, MQL conditions result in a significantly longer tool life across all tested parameters.

7. The EDX analysis corroborates the SEM findings, indicating that MQL conditions provide a more favorable environment for machining by reducing wear and extending tool life. The consistent presence of hard phases like WC and WC-TiC-TaC and the effective distribution of cobalt underscore the benefits of using MQL to improve the machinability and durability of carbide inserts.

Although the cooling environment significantly impacts all MCDM methods and is critical for improving machinability, this study limits its scope to just two cooling environments. Future research should explore other advanced cooling conditions, such as eco-friendly nanofluids with innovative application systems, to further improve machinability and promote sustainability. Additionally, incorporating more process parameters would allow for a more comprehensive optimization of machining responses. It is also essential to validate the reliability of proposed MCDM methods in other machining operations. Moreover, future studies should focus on comparing the correlations of MCDM methods within similar contexts to achieve more precise comparisons.

## Data availability statement

Data associated with this study has not been deposited in a publicly available repository. The data is included in the article.

## CRediT authorship contribution statement

**Nafisa Anzum Sristi:** Writing – review & editing, Writing – original draft, Visualization, Methodology, Investigation, Formal analysis, Data curation, Conceptualization. **Prianka B. Zaman:** Writing – review & editing, Supervision, Data curation, Conceptualization, Methodology. **Nikhil R. Dhar:** Supervision, Conceptualization, Data curation.

## Declaration of competing interest

The authors declare that they have no known competing financial interests or personal relationships that could have appeared to influence the work reported in this paper.

## References

[1] V.F. Sousa, F.J. Silva, Recent advances in turning processes using coated tools—a comprehensive review, Metals 10 (2) (2020) 170.
[2] T. Ogedengbe, et al., The effects of heat generation on cutting tool and machined workpiece, in: Journal of Physics: Conference Series, IOP Publishing, 2019.
[3] S. Yağmur, The effects of cooling applications on tool life, surface quality, cutting forces, and cutting zone temperature in turning of Ni-based Inconel 625, Int. J. Adv. Des. Manuf. Technol. 116 (3) (2021) 821–833.
[4] M.K. Gupta, et al., Comparison of tool wear, surface morphology, specific cutting energy and cutting temperature in machining of titanium alloys under hybrid and green cooling strategies, International Journal of Precision Engineering and Manufacturing-Green Technology 10 (6) (2023) 1393–1406.
[5] S. Debnath, M.M. Reddy, Q.S. Yi, Environmental friendly cutting fluids and cooling techniques in machining: a review, J. Clean. Prod. 83 (2014) 33–47.
[6] M. Najiha, M. Rahman, A. Yusoff, Environmental impacts and hazards associated with metal working fluids and recent advances in the sustainable systems: a review, Renew. Sustain. Energy Rev. 60 (2016) 1008–1031.
[7] M. Nazma Sultana, N. Ranjan Dhar, P. Binte Zaman, A review on different cooling/lubrication techniques in metal cutting, Am. J. Mech. Appl. 7 (4) (2019).
[8] M. Abas, et al., Optimization of machining parameters of aluminum alloy 6026-T9 under MQL-assisted turning process, J. Mater. Res. Technol. 9 (5) (2020) 10916–10940.
[9] A. Das, et al., Performance evaluation of various cutting fluids using MQL technique in hard turning of AISI 4340 alloy steel, Measurement 150 (2020) 107079.
[10] N. Sultana, N. Dhar, A critical review on the progress of MQL in machining hardened steels, Advances in Materials and Processing Technologies 8 (4) (2022) 3834–3858.
[11] N.S. Ross, et al., Thermo-physical, tribological and machining characteristics of Hastelloy C276 under sustainable cooling/lubrication conditions, J. Manuf. Process. 80 (2022) 397–413.
[12] M.E. Korkmaz, et al., Prediction and classification of tool wear and its state in sustainable machining of Bohler steel with different machine learning models, Measurement 223 (2023) 113825.
[13] N.S. Ross, et al., Development and potential use of MWCNT suspended in vegetable oil as a cutting fluid in machining of Monel 400, J. Mol. Liq. 382 (2023) 121853.
[14] M.K. Gupta, M.E. Korkmaz, A conceptual framework for sustainability impact assessment in machining bohler tool steel under hBN-enriched nano cutting fluids environment, Sustainable Materials and Technologies 37 (2023) e00669.
[15] R. Maruda, et al., Metrological analysis of surface quality aspects in minimum quantity cooling lubrication, Measurement 171 (2021) 108847.
[16] C. Divya, L.S. Raju, B. Singaravel, Application of MCDM methods for process parameter optimization in turning process—a review, Recent Trends in Mechanical Engineering: Select Proceedings of ICIME (2021) 199–207.
[17] M. Mia, et al., Taguchi S/N based optimization of machining parameters for surface roughness, tool wear and material removal rate in hard turning under MQL cutting condition, Measurement 122 (2018) 380–391.
[18] S. Rawat, Y. Zhang, C. Lee, Multi-response optimization of hybrid fibre engineered cementitious composite using Grey-Taguchi method and utility concept, Construct. Build. Mater. 319 (2022) 126040.
[19] P. Umamaheswarrao, et al., Application of TOPSIS for multi response optimization of Process Parameters in dry hard turning of AISI 52100 steel, Incas Bulletin 13 (1) (2021) 211–224.
[20] L.H. Li, R. Mo, Production task queue optimization based on multi-attribute evaluation for complex product assembly workshop, PLoS One 10 (9) (2015) e0134343.
[21] K.R. Arun Prasad, et al., Optimization of turning parameters for Magnesium Silicon Carbide using TOPSIS method, IOP Conf. Ser. Mater. Sci. Eng. 912 (3) (2020).
[22] R. Kumar, et al., Revealing the benefits of entropy weights method for multi-objective optimization in machining operations: a critical review, J. Mater. Res. Technol. 10 (2021) 1471–1492.
[23] V. Nguyen, T. Nguyen, D. Tien, Cutting parameter optimization in finishing milling of Ti-6Al-4V titanium alloy under MQL condition using TOPSIS and ANOVA analysis, Eng. Technol. Appl. Sci. Res. 11 (1) (2021) 6775–6780.
[24] S. Balasubramaniyan, T. Selvaraj, Application of integrated Taguchi and TOPSIS method for optimization of process parameters for dimensional accuracy in turning of EN25 steel, J. Chin. Inst. Eng. 40 (4) (2017) 267–274.

[25] R. Thirumalai, M. Seenivasan, K. Panneerselvam, Experimental investigation and multi response optimization of turning process parameters for Inconel 718 using TOPSIS approach, Mater. Today: Proc. 45 (2021) 467–472.
[26] A. Gupta, et al., Optimization of MQL machining parameters using combined Taguchi and TOPSIS method, in: Advances in Intelligent Manufacturing, Springer, 2020, pp. 93–101.
[27] D.T. Do, N.-T. Nguyen, Applying Cocoso, Mabac, Mairca, Eamr, Topsis and weight determination methods for multi-criteria decision making in hole turning process, J. Mech. Eng. 72 (2) (2022) 15–40.
[28] K. Abbed, et al., Effects of tool materials and cutting conditions in turning of Ti-6Al-4V alloy: statistical analysis, modeling and optimization using CoCoSo, MABAC, ARAS and CODAS methods, Int. J. Adv. Des. Manuf. Technol. 128 (3–4) (2023) 1535–1557.
[29] H. Yurtkuran, et al., Prediction of power consumption and its signals in sustainable turning of PH13-8Mo steel with different machine learning models, Int. J. Adv. Des. Manuf. Technol. (2024) 1–18.
[30] S.B. Patil, et al., Complex Proportional Assessment (COPRAS) based Multiple-Criteria Decision Making (MCDM) paradigm for hard turning process parameters, Mater. Today: Proc. 59 (2022) 835–840.
[31] M. Krishna, et al., Application of MOORA & COPRAS integrated with entropy method for multi-criteria decision making in dry turning process of Nimonic C263, Manuf. Rev. 9 (2022) 20.
[32] S. Das, et al., Optimization of CNC turning parameters of copper–nickel (Cu–Ni) alloy using VIKOR, MOORA and GRA techniques, Int. J. Interact. Des. Manuf. (2024) 1–10.
[33] M. Solanki, A. Jain, Optimization of material removal rate and surface roughness using Taguchi based multi-criteria decision making (MCDM) technique for turning of Al-6082, Proceedings on Engineering 3 (3) (2021) 303–318.
[34] M. Sarıkaya, A. Güllü, Multi-response optimization of minimum quantity lubrication parameters using Taguchi-based grey relational analysis in turning of difficult-to-cut alloy Haynes 25, J. Clean. Prod. 91 (2015) 347–357.
[35] B. Singaravel, T. Selvaraj, S. Vinodh, Multi-objective optimization of turning parameters using the combined moora and entropy method, Trans. Can. Soc. Mech. Eng. 40 (1) (2016) 101–111.
[36] S. Jeet, et al., Comparative investigation based on MOORA, GRA and TOPSIS method of turning of nickel-chromium-molybdenum steel under the influence of low cost oil mist lubrication system, Int. J. Appl. Eng. Res. 14 (13) (2019) 8–20.
[37] L.B. Abhang, M. Iqbal, M. Hameedullah, Optimization of machining process parameters using moora method, Defect Diffusion Forum 402 (2020) 81–89.
[38] S. Bag, et al., Optimization of turning process parameters on EN8 unalloyed steel-based on MCDM methods, Mater. Today: Proc. (2023).
[39] S. Hadjela, et al., Straight turning optimization of low alloy steel using MCDM methods coupled with Taguchi approach, Int. J. Adv. Des. Manuf. Technol. 124 (5) (2023) 1607–1621.
[40] S. Chauhan, et al., Parallel structure of crayfish optimization with arithmetic optimization for classifying the friction behaviour of Ti-6Al-4V alloy for complex machinery applications, Knowl. Base Syst. 286 (2024) 111389.
[41] M.E. Korkmaz, et al., Tool wear and its mechanism in turning aluminum alloys with image processing and machine learning methods, Tribol. Int. 191 (2024) 109207.
[42] N.R. Nazma Sultana, Dhar *Hybrid GRA-PCA and modified weighted TOPSIS coupled with Taguchi for multi-response process parameter optimization in turning AISI 1040 steel*, Arch. Mech. Eng. 58 (2021).
[43] N.A. Sristi, P.B. Zaman, N.R. Dhar, Multi-response optimization of hard turning parameters: a comparison between different hybrid Taguchi-based MCDM methods, Int. J. Interact. Des. Manuf. 16 (4) (2022) 1779–1795.
[44] P.B. Zaman, N.R. Dhar, Design and evaluation of an embedded double jet nozzle for MQL delivery intending machinability improvement in turning operation, J. Manuf. Process. 44 (2019) 179–196.
[45] S. Choudhury, N. Dhar, M. Bepari, Effect of minimum quantity lubricant on temperature chip and cutting force in turning medium carbon steel, Work 700 (800) (2007) 900.
[46] S. Ali, N. Dhar, S. Dey, Effect of minimum quantity lubrication (MQL) on cutting performance in turning medium carbon steel by uncoated carbide insert at different speed-feed combinations, Advances in Production Engineering & Management 6 (3) (2011).
[47] P.B. Zaman, S. Saha, N.R. Dhar, Hybrid Taguchi-GRA-PCA approach for multi-response optimisation of turning process parameters under HPC condition, Int. J. Mach. Mach. Mater. 22 (3–4) (2020) 281–308.
[48] S.K. Vaid, et al., Application of multi-criteria decision-making theory with VIKOR-WASPAS-Entropy methods: a case study of silent Genset, Mater. Today: Proc. 50 (2022) 2416–2423.
[49] E. Mulliner, N. Malys, V. Maliene, Comparative analysis of MCDM methods for the assessment of sustainable housing affordability, Omega 59 (2016) 146–156.
[50] D. Kumaran, S.S.S.S. Paramasivam, H. Natarajan, Optimization of high speed machining cutting parameters for end milling of AlSi7Cu4 using Taguchi based technique of order preference similarity to the ideal solution, Mater. Today: Proc. 47 (2021) 6799–6804.
[51] A. Khan, K. Maity, Parametric optimization of some non-conventional machining processes using MOORA method, Int. J. Eng. Res. Afr. 20 (2015) 19–40.
[52] A. Palanisamy, T. Selvaraj, Optimization of machining parameters for dry turning of incoloy 800H using Taguchi - based grey relational analysis, Mater. Today: Proc. 5 (2) (2018) 7708–7715.
[53] V. Kumar, et al., Application of SWARA-CoCoSo-based approach for tool selection of an electrical discharge machining process, Sustainable Production, Instrumentation and Engineering Sciences 1 (2023).
[54] V. Ganta, K.S. Sagar, D. Chakradhar, Multi objective optimisation of thermally enhanced machining parameters of Inconel 718 using grey relational analysis, Int. J. Mach. Mach. Mater. 19 (1) (2017) 57–75.
[55] M. Moradian, V. Modanloo, S. Aghaiee, Comparative analysis of multi criteria decision making techniques for material selection of brake booster valve body, J. Traffic Transport. Eng. 6 (5) (2019) 526–534.
[56] K.P. Kumar, V. Reddi, Significance of spearman's rank correlation coefficient, International Journal For Multidisciplinary Research 5 (4) (2023).
[57] S. Bandyopadhyay, Comparison among multi-criteria decision analysis techniques: a novel method, Progress in Artificial Intelligence 10 (2) (2021) 195–216.
[58] S.H. Mousavi-Nasab, A. Sotoudeh-Anvari, A comprehensive MCDM-based approach using TOPSIS, COPRAS and DEA as an auxiliary tool for material selection problems, Mater. Des. 121 (2017) 237–253.
[59] W. Sałabun, J. Wątróbski, A. Shekhovtsov, Are mcda methods benchmarkable? a comparative study of topsis, vikor, copras, and promethee ii methods, Symmetry 12 (9) (2020) 1549.
[60] J. Więckowski, Z. Szyjewski, Practical study of selected multi-criteria methods comparison, Proc. Comput. Sci. 207 (2022) 4565–4573.
[61] M. Elbah, et al., Comparative assessment of machining environments (dry, wet and MQL) in hard turning of AISI 4140 steel with CC6050 tools, Int. J. Adv. Des. Manuf. Technol. 105 (5) (2019) 2581–2597.
[62] S. Swain, et al., Machinability performance investigation in CNC turning of Ti–6Al–4V alloy: dry versus iron-aluminium oil coupled MQL machining comparison, International Journal of Lightweight Materials and Manufacture 5 (4) (2022) 496–509.
[63] N. Barari, S.A. Niknam, H. Mehmanparast, Tool wear morphology and life under various lubrication modes in turning stainless steel 316L, Trans. Can. Soc. Mech. Eng. 44 (3) (2019) 352–361.